Coulomb blockade in quantum dots

L. I. Glazman

University of Minnesota

Charge Quantization

Outline

1. Early experiments on charge quantization and Coulomb blockade
2. Energy scales of a closed quantum dot
3. Electron transport: effects of charge quantization
4. Statistical description of the discrete electron states in the dot
5. Mesoscopic fluctuations of the conduction through a dot

Indirect evidence of charging effects:

C. J. Gorter, Physica 17, 777 (1951)

C. A. Neugebauer, M. B. Webb, J. Appl. Phys. 33, 74 (1962)

hopping (in-plane conductivity) in granular films

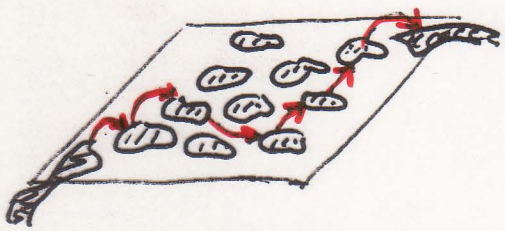

Clear demonstration of the role of charging: "vertical" tunneling through a layer of grains:

I. Giaever, H. R. Zeller, PRL 20, 1504 (68), Phys. Rev (1969)

J. Lambe, R. C. Jaklevic, PRL 22, 1371 (1969)

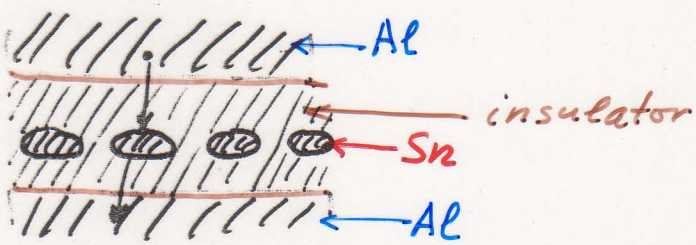

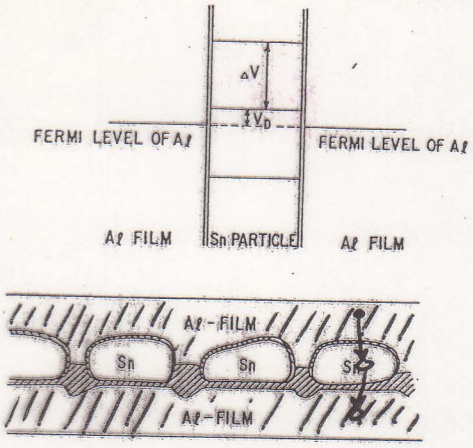

FIG. 1. Model and level scheme of Sn particles in a tunnel junction. V_D is the energy in eV of the last filled state at $T=0$ of the Sn particle, with respect to the Fermi energy of Al. $\Delta V = e/C$ is the voltage change of the particle caused by addition of one electron. In equilibrium $-e/2C \geq V_D \geq e/2C$ holds.

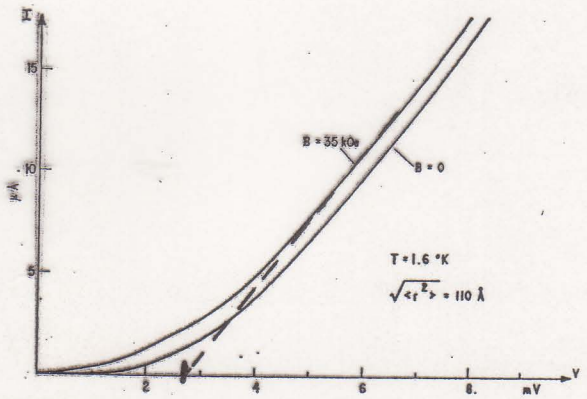

FIG. 7. Current-versus-voltage characteristic of a junction with average particle radius $r=110$ Å at 1.6°K for $H=0$ (particles superconducting) and $H=35$ kOe (particles normal).

When a voltage is applied we get a current flow through the junction. The electrons can flow from one side of the junction to the other by essentially three different mechanisms:

(1) direct tunneling through the aluminum oxide, avoiding the Sn particles. This mechanism gives a constant, voltage- and temperature-independent, background conductivity. For properly prepared junctions with a particle radius $r>30$ Å direct tunneling can be made completely negligible even at 1°K and at zero bias.

(2) tunneling from one Al film onto a Sn particle, localizing the electron there and then in turn tunneling out on to the other side. This process needs an activation energy which in turn is responsible for the zero-bias resistance peak. We will discuss this process in most of the remainder of the paper.

(3) tunneling from one aluminum film through a particle and out onto the other aluminum film without actually localizing the electron on the particle. The particle is only involved as an intermediate state; thus, the process is of second order. This process can conceivably become important at low temperatures and at low voltages; however, no experimental evidence has been found for this process. It is very similar in principle to Anderson's model[18] for tunneling involving intermediate magnetic impurity states.

According to process (2), in order to get a current flow the number of electrons on a Sn particle has to be changed by at least one. The activation energy required is equal to the difference of the Coulomb energies in the initial and the final state, i.e.,

$$E=\tfrac{1}{2}(e/C \pm V_D)^2 C - \tfrac{1}{2} V_D^2 C, \qquad (1)$$

where the positive sign holds for adding an electron and the negative sign for subtracting an electron. This activation energy can only be supplied by the battery. We would like to emphasize again that E is a pure classical Coulomb energy, and that all effects due to the level spacing in the particle have been neglected since the level spacing is small compared with E.

The capacitance of a specific particle, C, is simply the sum of the capacitance between the particle and the

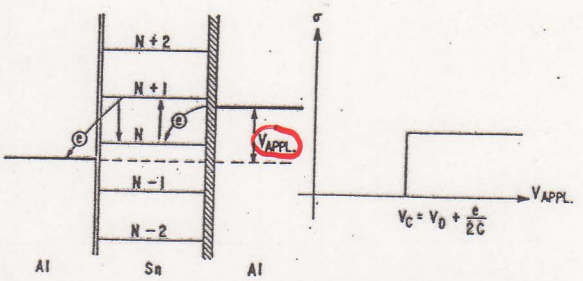

FIG. 13. Mechanism of current flow for an asymmetric junction ($C_L \gg C_R$). An electron from the right film tunnels into the particle, raising its electron number from N to $N+1$ and its voltage from V_D to V_D+e/C. In a next step the electron tunnels out onto the left film bringing the particle back in its ground state. This results in a step function for the conductivity as a function of voltage.

$$\Delta E_N = \frac{(N+1)^2 e^2}{2C} - \frac{N^2 e^2}{2C} = \frac{2N+1}{2C} e^2$$

$$eV_{APPL}^{(N)} \simeq \Delta E_N = (2N+1)\frac{e^2}{2C}$$

sequential tunneling

co-tunneli

similar with Anderson impurity model

Observation of Single-Electron Charging Effects in Small Tunnel Junctions

T. A. Fulton and G. J. Dolan
AT&T Bell Laboratories, Murray Hill, New Jersey 07974
(Received 6 March 1987)

Unusual structure and large electric-field–induced oscillations have been observed in the current-voltage curves of small-area tunnel junctions arranged in a low-capacitance ($\lesssim 1$ fF) multiple-junction configuration. This behavior arises from the tunneling of individual electrons charging and discharging the capacitance. The observations are in accord with what would be expected from a simple model of the charging energies and voltage fluctuations of e/C associated with such effects.

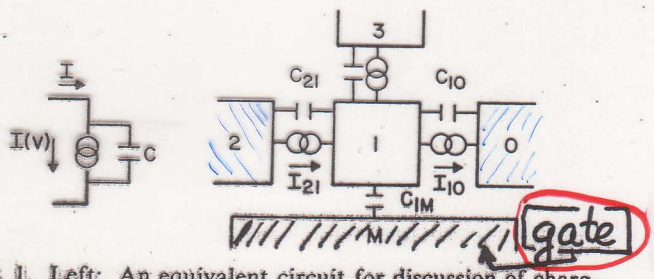

IG. 1. Left: An equivalent circuit for discussion of charg- effects for a single junction. Right: A comparable triple- tion circuit model.

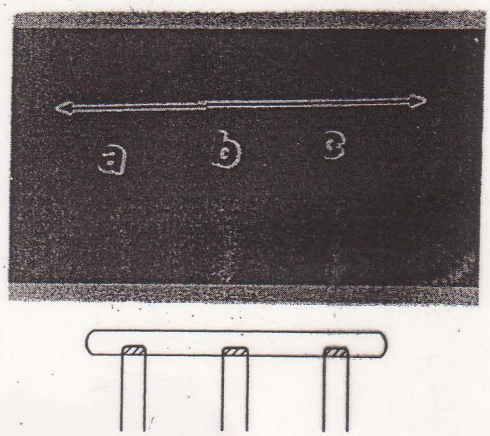

FIG. 2. A scanning-electron micrograph of a typical sample. Junctions labeled a, b, and c are formed where the vertical electrodes overlap and contact the longer horizontal central electrode. The bar is 1 μm long. The configuration is also shown in the accompanying drawing.

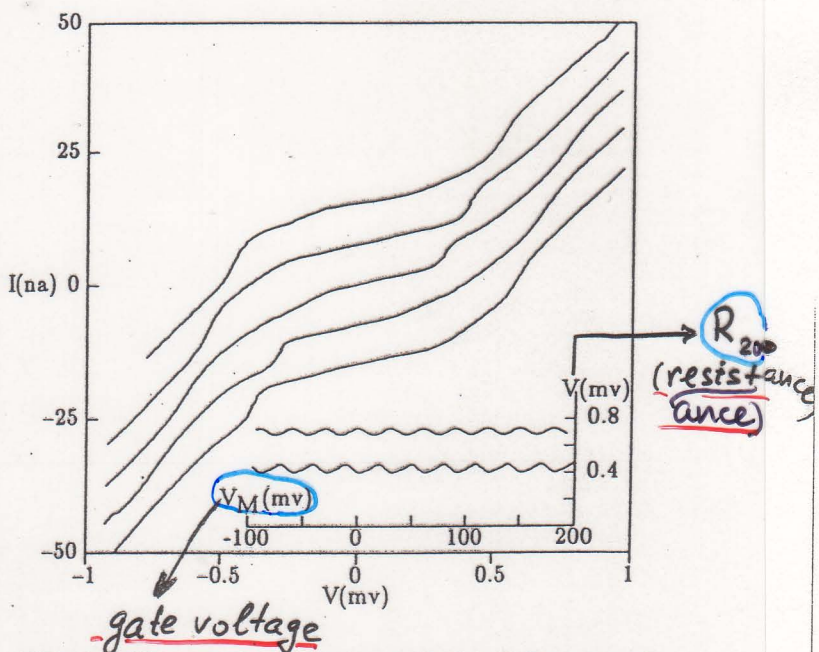

FIG. 5. I-V curves for a sample at $T=1.1$ K for a set of equally spaced substrate biases covering $\frac{5}{6}$ of a cycle. Curves are offset by increments of 7.5 nA. Inset: V vs V_M for two fixed currents $I=10.5$ and 26 nA.

Quantum dot ≡ mesoscopic puddle of electron liquid

$L \gg \lambda_F$

* Dominant energy scale: charging

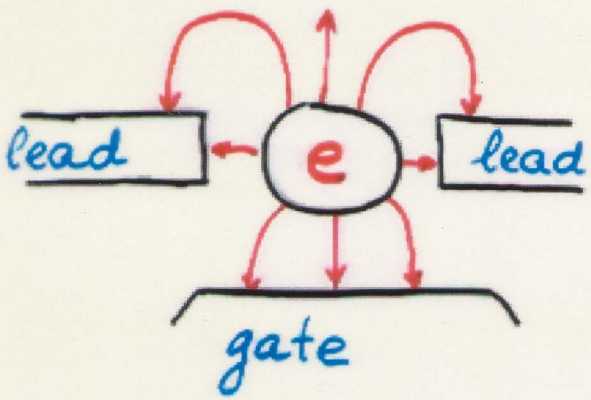

$$E_c = \frac{e^2}{2C}, \qquad C \sim L$$

* Smaller energy scale: discrete level spacing

$$\delta E = \frac{1}{\nu L^d}$$

$$\frac{\delta E}{E_c} = \frac{\hbar v_F}{e^2} \cdot \frac{1}{(k_F L)^{d-1}} \simeq \frac{1}{r_s} \cdot \frac{1}{(k_F L)^{d-1}} \ll 1$$

($d \equiv$ dimension)

Charge of a quantum dot

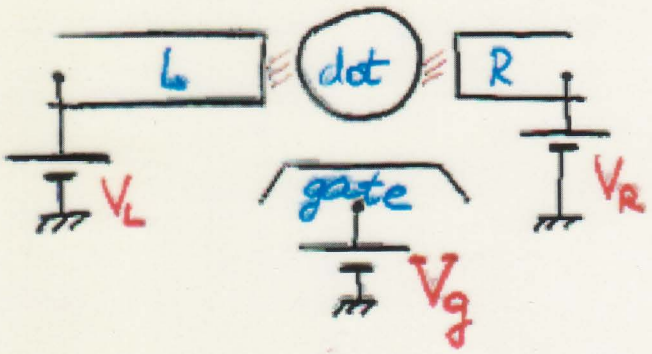

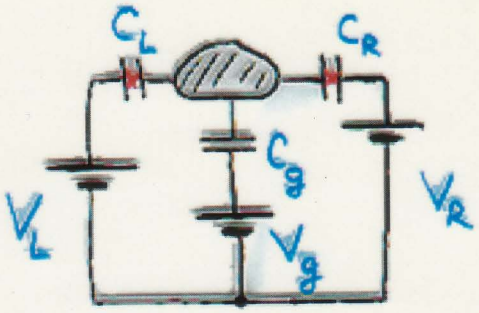

Electrostatic energy: $E(\hat{N}) = E_c \cdot (\hat{N} - \mathcal{N})^2$,

$\mathcal{N} \equiv V_g / eC_g$

min [E(N)]: $N = \mathcal{N}$ for continuous N

Discrete N: staircase

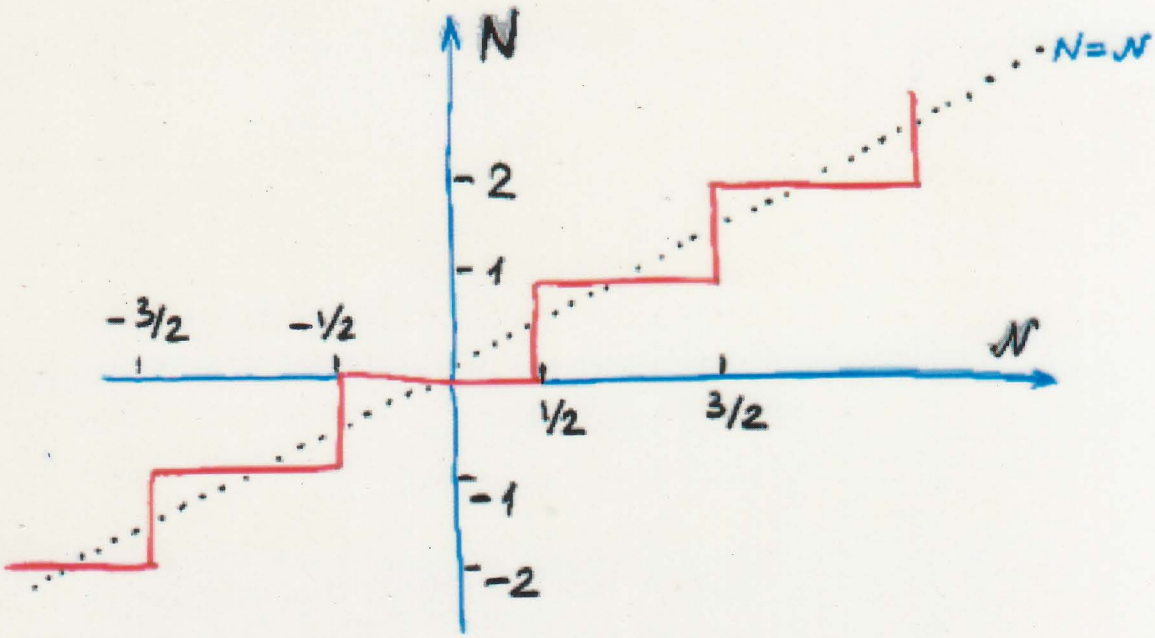

August 3, 1993

LT-20

MEASUREMENT OF THE INCREMENTAL CHARGE OF A SUPERCONDUCTING ISLAND

D. Esteve, P. Lafarge, P. Joyez, C. Urbina and M.H. Devoret

Service de Physique de l'Etat Condensé, CEA-Saclay

F 91191 Gif-sur-Yvette, France

$\frac{\Delta}{e} \simeq 180\,\mu V$

$\frac{1}{e}(\Delta - E_c) \simeq 10\,\mu V$

$T = 28\,mK$

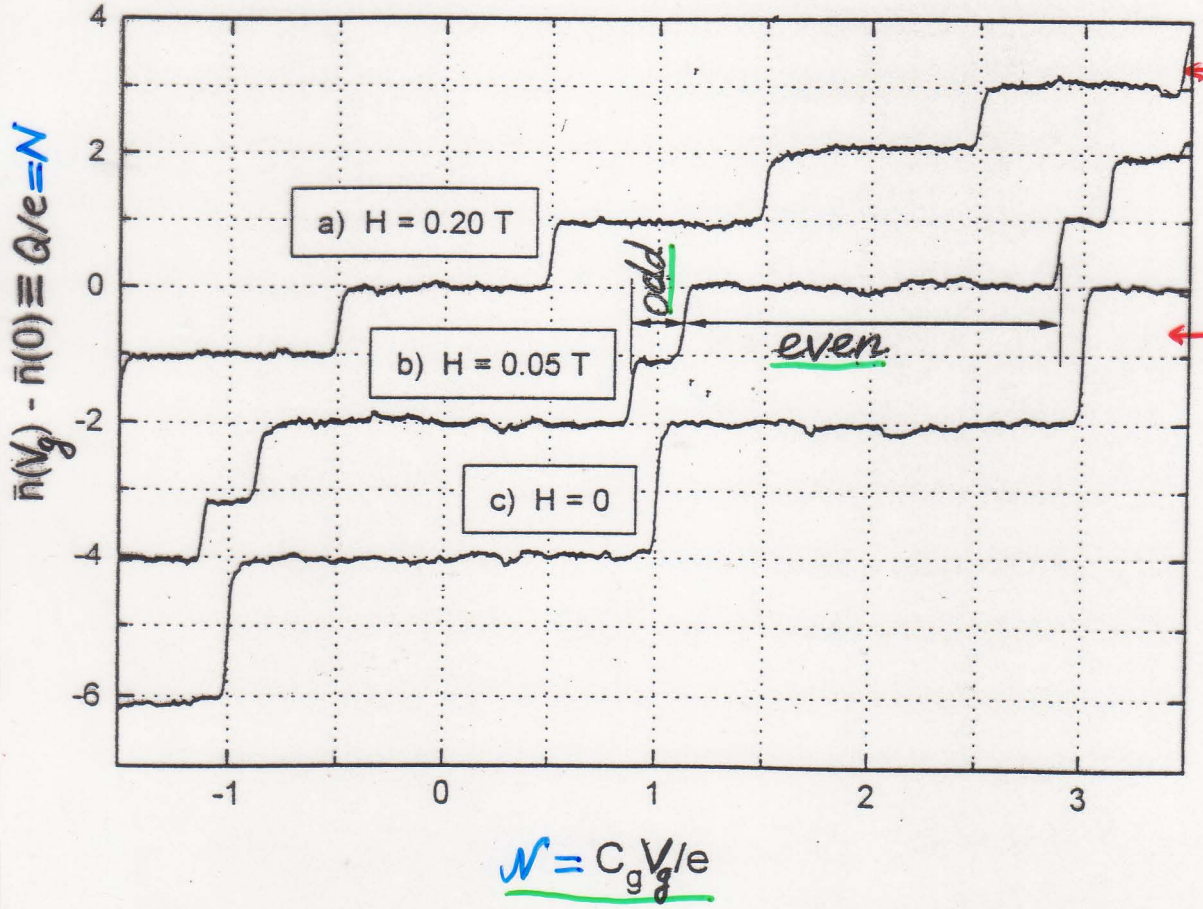

Fig. 4

Tunneling rate

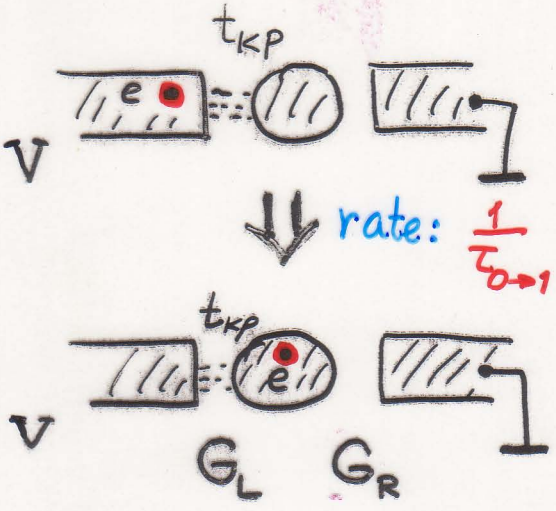

Probability of no extra electron on the dot: W_0

$$W_0 + W_1 = 1$$

Rate:

$$\frac{1}{\tau_{0\to 1}} = W_0 \frac{2\pi}{\hbar} \sum_{k,p} |t_{kp}|^2 n_k (1-n_p)\, \delta(\varepsilon_k + eV + E_0 - \varepsilon_p - E_1)$$

$$= W_0 \cdot \frac{1}{e^2} \cdot G_L \, f(E_1 - E_0 - eV)$$

$$f(x) = \frac{x}{e^{x/T} - 1}, \qquad x = \underbrace{E_1}_{\text{electrostatic energies}} - \underbrace{E_0}_{\text{electrostatic energies}} - eV$$

In the equilibrium (Gibbs):

$$W_0 = \frac{f(E_0 - E_1)}{f(E_0 - E_1) + f(E_1 - E_0)}$$

$$W_1 = \frac{f(E_1 - E_0)}{f(E_0 - E_1) + f(E_1 - E_0)}$$

Balance equation:

$$G_L\left[W_0 f(E_1-E_0-eV) - W_1 f(E_0-E_1+eV)\right] =$$

$$= \underbrace{G_R\left[W_1 f(E_0-E_1) - W_0 f(E_1-E_0)\right]}_{\text{current through the right junction}}$$

Linear conductance ($eV \to 0$):

$$G = \frac{G_L G_R}{G_L+G_R} \cdot \frac{f(\varepsilon) f'(-\varepsilon) + f'(\varepsilon) f(-\varepsilon)}{f(\varepsilon) + f(-\varepsilon)}$$

$\varepsilon = E_1 - E_0$ depends on V_g

* equilibration between tunneling events
* independent $\Rightarrow$ tunneling through G_L, G_R

Characteristic temperature: E_c.

At $T \ll E_c$, and assuming $\delta E \to 0$

$$G(N,T) = \frac{1}{2R_\infty} \cdot \frac{2E_c(N-N^*)/T}{\sinh\left[2E_c(N-N^*)/T\right]} \quad , \quad N \equiv \frac{V_g}{eC_g}$$

$$N^* \equiv n + \tfrac{1}{2}$$

(L.G., Shekhter 1989)

R_∞ - "usual" high-T value of resistance for two tunnel junctions in series:

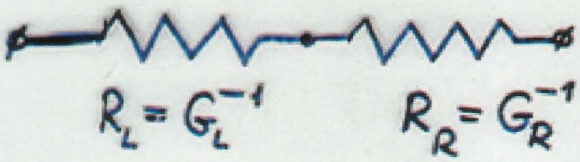

$$R_\infty = R_L + R_R = \frac{G_L + G_R}{G_L G_R}$$

In the limit $T \to 0$ conductance $G(N,T) \to$ (exponentially) 0 at all N except isolated points of charge degeneracy $N^* \equiv n + \frac{1}{2}$

In the continuous spectrum approx.,
all peaks have the same amplitude, $G_{max} = \frac{1}{2R_\infty}$

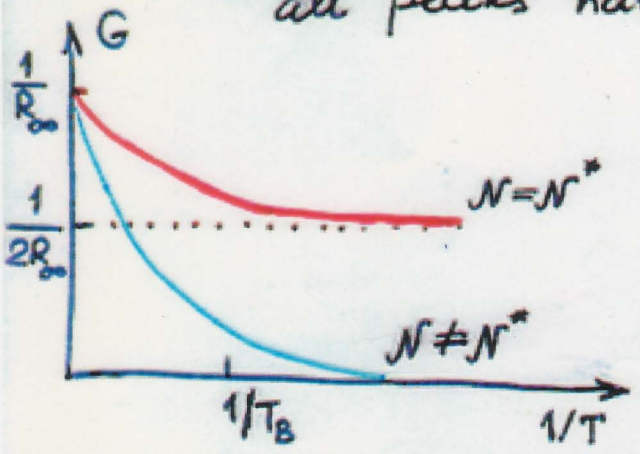

(e-like or h-like degeneracy)

Strong Tunneling in the Single-Electron Transistor

P. Joyez, V. Bouchiat, D. Esteve, C. Urbina, and M. H. Devoret
Service de Physique de l'Etat Condensé, Commissariat à l'Energie Atomique, Saclay, 91191 Gif-sur-Yvette, France
(Received 27 January 1997)

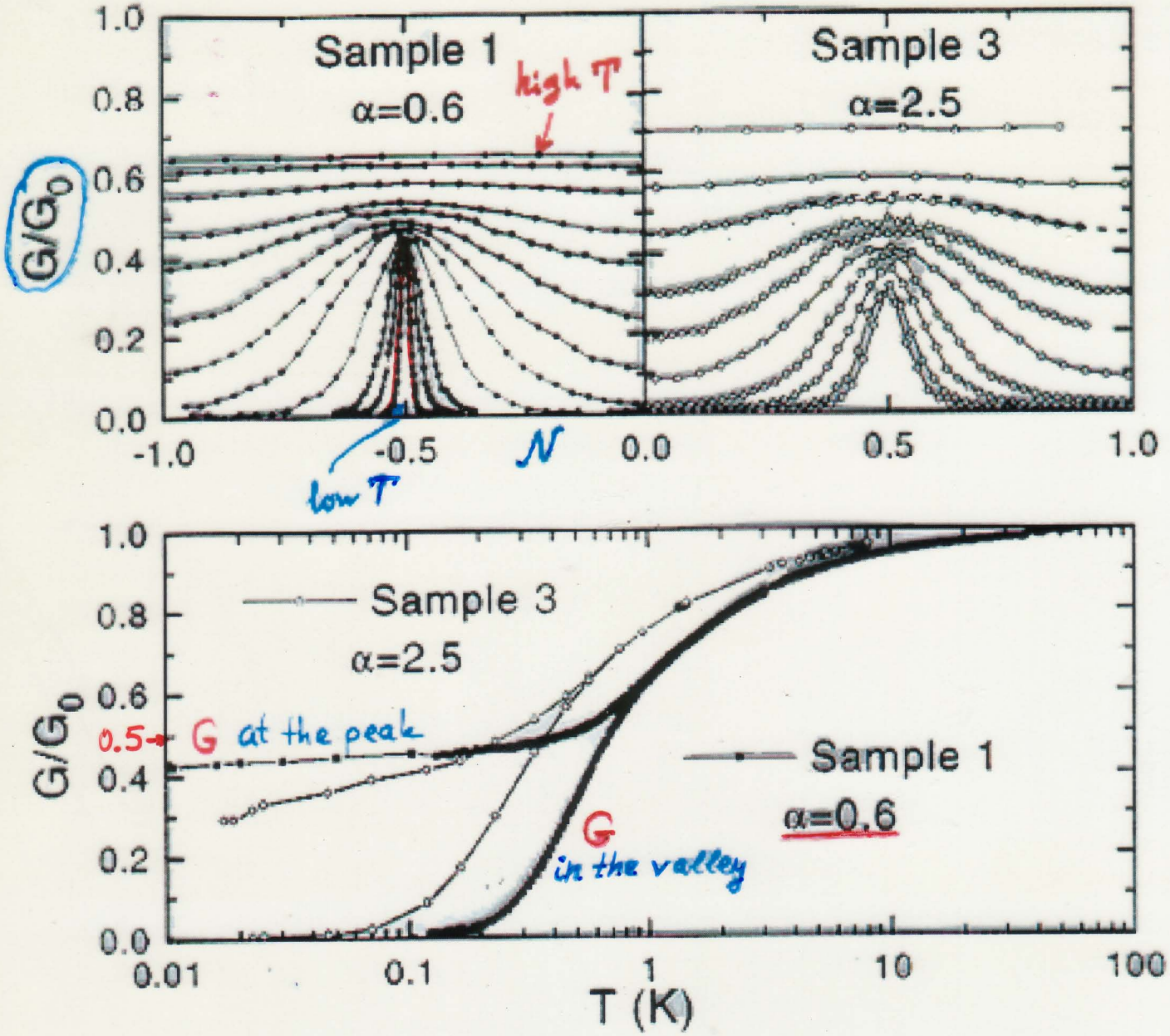

PRL 77, No 17 (1996)
Kouwenhoven, Tarucha

Transport Spectroscopy

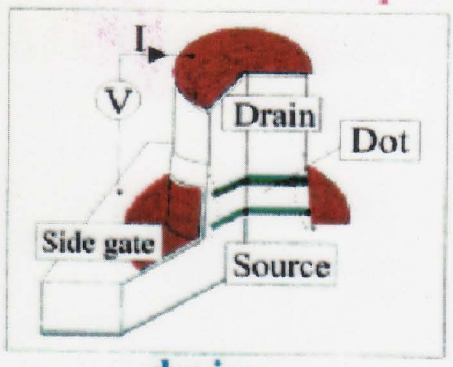

device

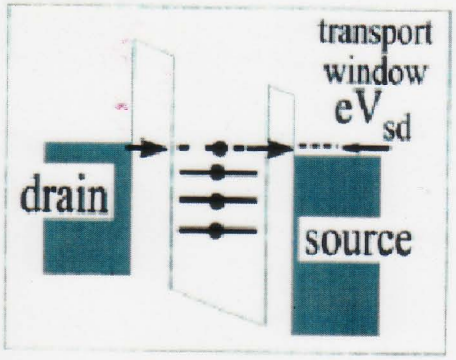

single electron tunneling

- ***charging energy e^2/C***
  (ionization energy)
- ***discrete energy levels***
  (excitation energy)

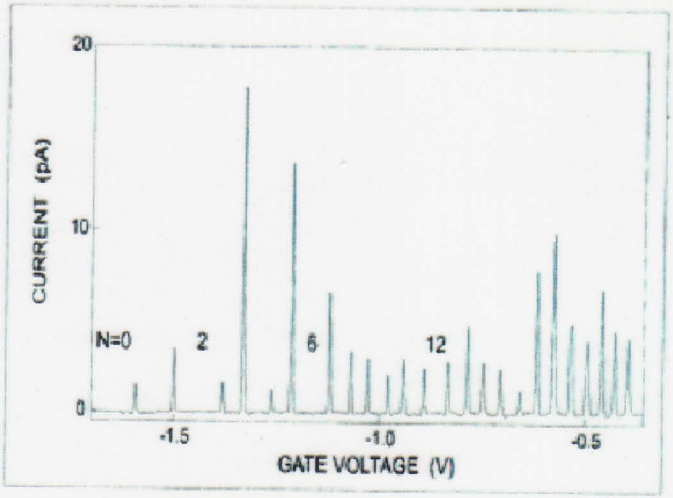

Coulomb oscillations

Statistics of Coulomb Blockade Peak Spacings

S. R. Patel, S. M. Cronenwett, D. R. Stewart, A. G. Huibers, and C. M. Marcus
Department of Physics, Stanford University, Stanford, California 94305

C. I. Duruöz and J. S. Harris, Jr.
Electrical Engineering Department, Stanford University, Stanford, California 94305

K. Campman and A. C. Gossard
Materials Department, University of California at Santa Barbara, Santa Barbara, California 93106
(Received 5 August 1997)

Distributions of Coulomb blockade peak spacings are reported for large ensembles of both unbroken (magnetic field $B = 0$) and broken ($B \neq 0$) time-reversal symmetry in GaAs quantum dots. Both distributions are symmetric and roughly Gaussian with a width of ~2%–6% of the average spacing, with broad, non-Gaussian tails. The distribution is systematically wider at $B = 0$ by a factor of $\sim 1.2 \pm 0.1$. No even-odd spacing correlations or bimodal structure in the spacing distribution is found, suggesting an absence of spin degeneracy. There is no observed correlation between peak spacing and peak height. [S0031-9007(98)06083-9]

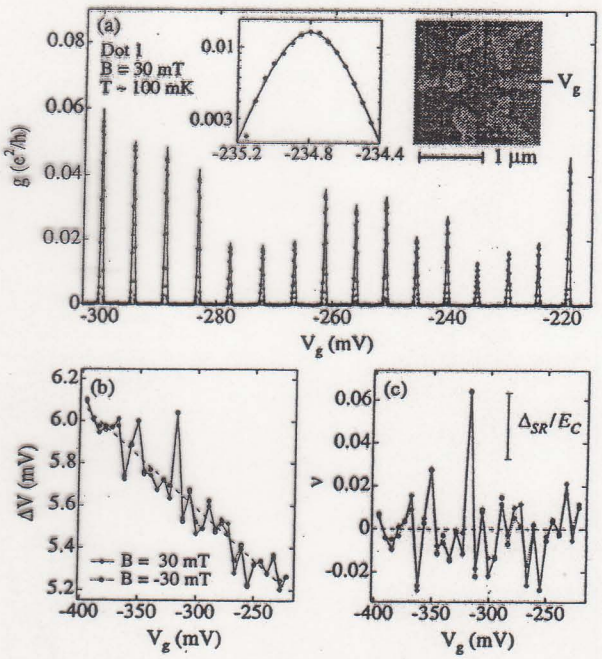

FIG. 1. (a) Coulomb blockade peaks (diamonds) at $B = 30$ mT as a function of gate voltage V_g for device 1 with $\Delta_{SR} = 14$ μeV and $E_C = 460$ μeV. Solid curve shows fits to $\cosh^{-2}$ line shape. Left inset: Detailed view of data and fit on log-linear scale. Right inset: Micrograph of device 1; other devices are similar. (b) Peak spacings extracted from data in (a) at $B = +30$ mT (diamonds) and $B = -30$ mT (open circles). Dashed line is best fit (to +30 mT data), corresponding to $\langle \Delta V_g^i \rangle$. (c) Dimensionless peak spacing fluctuations, $\nu = (\Delta V_g^i - \langle \Delta V_g^i \rangle)/\langle \Delta V_g^i \rangle$, as a function of gate voltage V_g for data in (b). Differences between ± 30 mT data indicated experimental noise. Normalized (spin-resolved) mean level spacing Δ_{SR}/E_C indicated by vertical bar (see Table I).

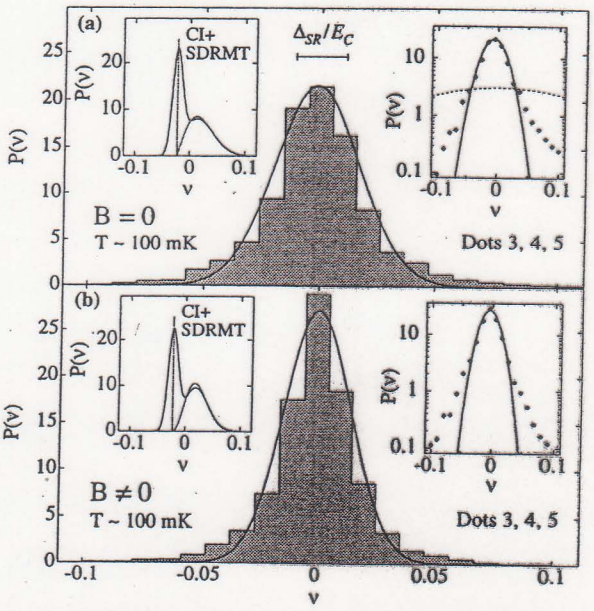

FIG. 2. Histograms of normalized peak spacing ν (bars) for (a) $B = 0$ and (b) $B \neq 0$ for devices 3, 4, and 5. Solid curves show best fit to normalized Gaussian of width 0.019 (0.015) for $B = 0$ ($B \neq 0$). The $B = 0$ histogram is wider by a factor of ~1.2 than the $B \neq 0$ histogram. Data represent 4300 (10 800) CB peaks from the devices with ~720 (1600) statistically independent for $B = 0$ ($B \neq 0$). Horizontal bar indicates (spin-resolved) mean level spacing Δ_{SR}/E_C averaged over the three devices. Right insets: Plots of histogram (diamonds) and best fit Gaussian (solid curve) on log-linear scale. Dashed curve is Gaussian of width 0.13 from Ref. [5]. Left insets: Dotted curves are CI + SDRMT peak spacing distributions; solid curves correspond to CI + SDRMT distributions convolved with Gaussian of width $\sigma_{noise}(\nu) = 0.009$ averaged over the three dots (see Table I).

Models of an isolated quantum dot

1. The Constant-Interaction (CI) model:

accounts for the scales E_c and δE

$$\mathcal{H}_{CI} = \sum_{n,\sigma} \xi_n d^+_{n\sigma} d_{n\sigma} + E_c (\hat{N} - N)^2 ;$$

$$\hat{N} = \sum_{n,\sigma} d^+_{n\sigma} d_{n\sigma} .$$

Spin of the dot is $S = 0$ if N = even, and

$S = 1/2$ if N = odd.

2. The Universal Hamiltonian (CIE model):

accounts for E_c, δE, and the

intra-dot exchange E_s

$$\mathcal{H}_{CIE} = \mathcal{H}_{CI} - E_s \hat{S}^2_{dot} ; \quad E_s \sim r_s \delta E$$

(r_s is the gas parameter) [Kurland, Aleiner, Altshuler PRB'00; Aleiner, Brouwer, L.G. cond-mat/0103008] → Phys. Rep. 358, No.5-6 (2002)

The dot may have $S \neq 0$ in a state with N = even

[Oreg, Brouwer, Halperin PRB'99; Ullmo, Baranger, L.G. PRB'00]

Description of free fermions in a disordered dot: the idea of Random Matrix Theory (RMT)

$$\mathcal{H}_F = \sum_i \xi_i d_i^\dagger d_i$$

$$\hat{d}_i = \int_{dot} d\vec{r}\ \hat{\Psi}(\vec{r})\,\varphi_i^*(\vec{r})$$

$$\left[-\frac{\nabla^2}{2m} + U(\vec{r}) \right] \varphi_i(\vec{r}) = \xi_i\, \varphi_i(\vec{r})$$

$$\int_{dot} d\vec{r}\ |\varphi_i(\vec{r})|^2 = 1$$

Statistical properties of φ_i, ξ_i are important

Universal properties of spectrum ξ_i

$$G^{R/A}(\varepsilon, \vec{r}_1, \vec{r}_2) = \sum_i \frac{\varphi_i^*(\vec{r}_2)\,\varphi_i(\vec{r}_1)}{\varepsilon - \xi_i \pm i0}$$

$$\nu(\varepsilon) \underset{def.}{=\!=} \sum_i \delta(\varepsilon - \xi_i) = \frac{1}{2\pi i} \int d\vec{r} \left[G^A(\varepsilon, \vec{r}, \vec{r}) - G^R(\varepsilon, \vec{r}, \vec{r}) \right]$$

$$\frac{1}{\delta E} \equiv \langle \nu(\varepsilon) \rangle$$

↑ average (ensemble or energy)

Universal properties of spectrum

$$R^{(2)}(\omega) = (\delta E)^2 \langle \nu(\varepsilon)\nu(\varepsilon+\omega)\rangle - 1$$

$$= \frac{(\delta E)^2}{2\pi^2}\, \mathrm{Re} \int d\vec{r}_1\, d\vec{r}_2 \langle G^R(\varepsilon+\omega, \vec{r}_1, \vec{r}_1)\, G^A(\varepsilon, \vec{r}_2, \vec{r}_2)\rangle - 1$$

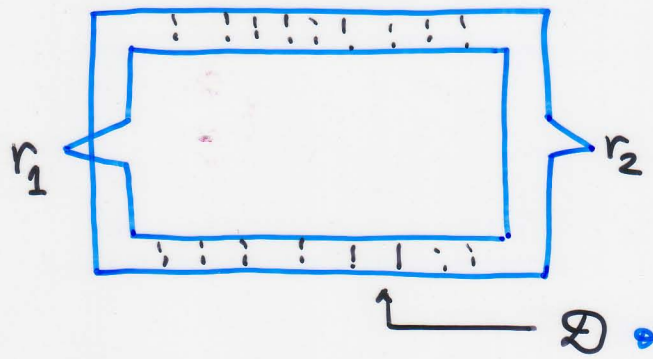

$|\vec{r}_1 - \vec{r}_2| \sim L \gg \lambda_F$

[Altshuler, Shklovskii 86]

$$\langle G^R(\varepsilon+\omega, r_1, r_1)\, G^A(\varepsilon, r_2, r_2)\rangle - \nu^2 \sim \underbrace{\mathcal{D}^2}_{\text{"strong" } B} \text{ or } \underbrace{\mathcal{D}^2 + C^2}_{B=0}$$

$$\left[-i\omega + D(-i\nabla)^2\right] \mathcal{D}_\omega = \delta(\vec{r}_1 - \vec{r}_2)\,, \qquad \left.\frac{\partial \mathcal{D}}{\partial \vec{n}}\right|_{\text{boundary}} = 0$$

(D: diffusion constant)

Eigenvalue problem: $-D\nabla^2 f_n = \gamma_n f_n\,, \qquad \frac{\partial f}{\partial \vec{n}} = 0$

$\gamma_0 = 0\,, \quad f_0 \sim \frac{1}{L^2}\,; \qquad \gamma_1 \equiv E_T \sim \frac{D}{L^2}$ ← Thouless energy

$$R^{(2)}(\omega) = -\frac{(\delta E)^2}{\beta \pi^2 \omega^2} + \frac{(\delta E)^2}{\beta \pi^2}\, \mathrm{Re} \sum_{\gamma_n \neq 0} \frac{1}{(i\omega + \gamma_n)^2}$$

universal — small, $\sim (\delta E / E_T)^2$

$$\beta = \begin{cases} 1, & B = 0 \\ 2, & B \neq 0 \end{cases}$$

$$\delta E \ll \omega \ll E_T$$

All statistical properties of spectrum at $\omega \ll E_T$ are equivalent to that of random matrix Hamiltonian

$$\mathcal{H}_F = \sum_{ij} h_{ij}\, d_i^+ d_j$$

h_{ij} : matrix elements of $\hat{\mathcal{H}}$

$$P\{\hat{\mathcal{H}}\} = C \exp\{-A \cdot \mathrm{Tr}(\hat{\mathcal{H}}^2)\}$$

$$\langle h_{ij}\, h_{i'j'} \rangle = \frac{M(\delta E)^2}{\pi^2}\left[\delta_{ij}\delta_{i'j'} + \left(\frac{2}{\beta} - 1\right)\delta_{ii'}\delta_{jj'}\right]$$

$$\beta = \begin{cases} 1 & \text{Gaussian Orthogonal Ensemble (GOE), } B = 0 \\ 2 & \text{Unitary} \qquad \underline{\text{GUE}}, \; B \gtrsim \Phi_0/L^2 \end{cases}$$

$$M \gtrsim \frac{E_T}{\delta E} \equiv g, \quad \text{dimensionless conductance}$$

$g \gg 1$

$$G \sim \frac{e^2}{h} \cdot g$$

* Crossover (GOE → GUE) field (flux Φ_c)

Energy scale $\omega \to$ time $t \sim 1/\omega$. Area covered in diffusion $\sim Dt$. Winding number (random) $\sim \pm\sqrt{Dt/L^2}$.

Threading flux : $\sim \sqrt{Dt/L^2} \cdot L^2 \cdot B \sim \sqrt{E_T/\omega}\,\Phi$

Def. of Φ_c depends on ω: $\boxed{\sqrt{E_T/\omega}\,\Phi_c^{(\omega)} \equiv \Phi_0}$

$$\omega \sim \delta E \Rightarrow \Phi_c = \Phi_0/\sqrt{g}$$

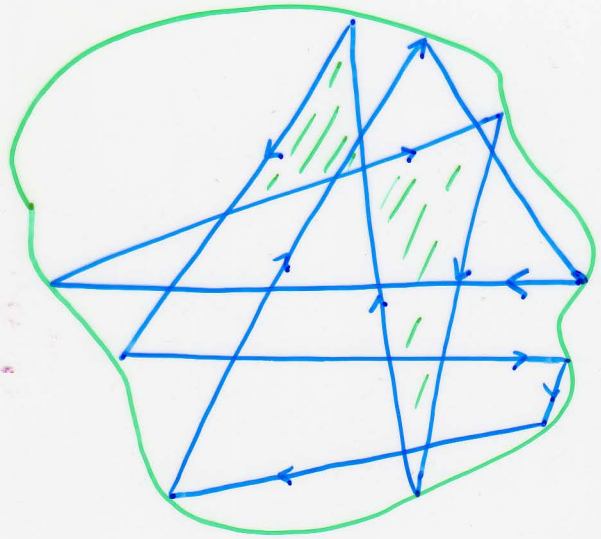

$$\Phi = \int \vec{A} \cdot d\vec{\ell}$$

Statistics of eigenstates in RMT

Level spacing distribution (Wigner-Dyson)

$$P(\xi) = \begin{cases} (\pi/2)\,\xi \exp\left(-\frac{\pi}{4}\xi^2\right) & \text{GOE} \\ (32/\pi^2)\,\xi^2 \exp\left(-\frac{4}{\pi}\xi^2\right) & \text{GUE} \end{cases} \qquad \xi = \xi_n - \xi_{n-1}$$

Statistics of eigenvectors (Porter-Thomas)

$$P(\{c_i\}) = \text{const} \cdot \delta\left(1 - \sum_{i=1}^{M} |c_i|^2\right) \quad \text{(symmetry of } P\{\hat{\mathcal{H}}\}\text{)}$$

$$\eta \equiv M|c_i|^2$$

$$P(\eta) = \begin{cases} \frac{1}{\sqrt{2\pi\eta}} e^{-\eta/2} & \text{GOE} \\ e^{-\eta} & \text{GUE} \end{cases} \qquad M \to \infty$$

$$\varphi_n = \{c_i^{(n)}\} \qquad \langle \varphi_n \varphi_m^* \rangle \propto \delta_{nm} \quad \text{GOE or GUE}$$

Real space: $P(|\varphi_n(\vec{r})|^2)$ - Porter-Thomas distr.

$$\langle \varphi_n(\vec{r}_1) \varphi_m^*(\vec{r}_2) \rangle \propto \delta_{nm}$$

---

* GOE $\leftrightarrow$ GUE within $|\varepsilon| \sim \omega$: $\Phi_c^{(\omega)} \sim \Phi_0 \sqrt{E_T/\omega}$; $\omega \sim \delta E \div E_T$

* RMT is sensible if $g = \frac{E_T}{\delta E} \gg 1$

* Diffusive $\rightarrow$ ballistic $E_T \sim \frac{D}{L^2} \rightarrow E_T \sim \frac{v_F}{L}$

* Ballistic 2D: $g \sim \sqrt{N}$ ← number of electrons in a dot

Porter-Thomas distribution for neutron widths Γ

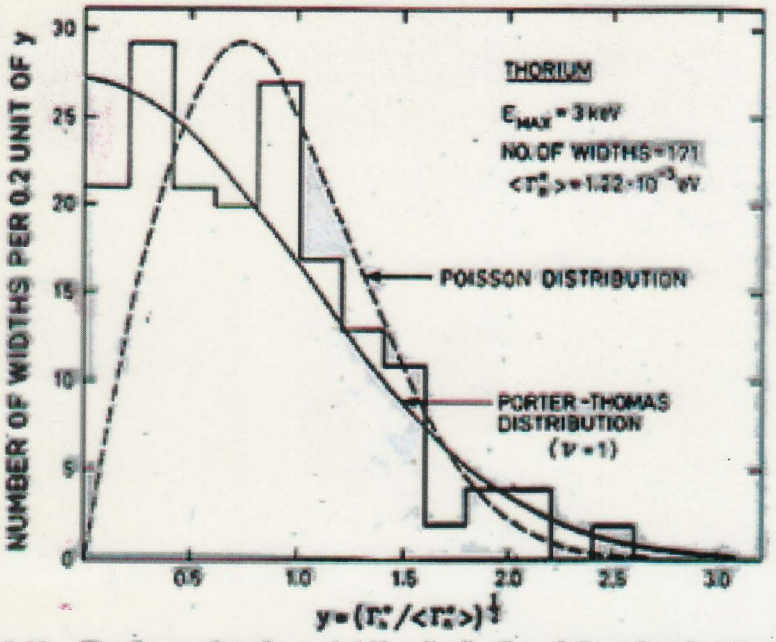

Figure 2-10 The figure plots the probability distribution of the reduced neutron widths observed in the reaction $n + {}^{232}\text{Th}$ ($\Gamma_n^{o}(E_r) = \Gamma_n(E_r)E_r^{-1/2}$(eV)). The data are taken from J. B. Garg, J. Rainwater, J. S. Petersen, and W. W. Havens, Jr., *Phys. Rev.* 134, B985 (1964).

▼ The theoretical distribution obtained in the limit of extreme configuration mixing (Porter and Thomas, 1956) is a χ^2 distribution with $\nu = 1$. Since such a distribution varies as $(\Gamma_n^{o})^{-1/2}$ for small values of Γ_n^{o} (see Eq. (2C-28)),

$$P(\Gamma_n^{o}) = (2\pi\Gamma_n^{o}\langle\Gamma_n^{o}\rangle)^{-1/2}\exp\left(-\frac{\Gamma_n^{o}}{2\langle\Gamma_n^{o}\rangle}\right) \qquad (2\text{-}115)$$

it is convenient to plot the distribution of $(\Gamma_n^{o})^{1/2}$. The observed widths in Fig. 2-10 follow the distribution (2-115) rather well, but are in disagreement with the Poisson distribution (a χ^2 distribution with $\nu = 2$; see Eq. (2C-29)).

Compound nucleus state $\equiv$ (normalised) random vector of large dimension

Neutron width $\propto$ square of one component of this vector

$$P(c_1,\ldots,c_N) = \frac{2}{\Omega_N}\,\delta\left(1-\sum_{i=1}^{N}c_i^2\right), \qquad \Omega_N = \frac{N\pi^{N/2}}{\Gamma\left(\frac{N}{2}+1\right)}$$

$$P(c_1) \simeq \sqrt{\frac{N}{2\pi}}\exp\left\{-\frac{N}{2}c_1^2\right\} \qquad P(c)\,dc = \frac{1}{2c}P(c^2)\,dc^2$$

$$P_{PT}(\Gamma) \propto P(c_1^2) \propto \frac{1}{\langle c_1^2\rangle^{1/4}\,c_1^{1/2}}\exp\left\{-\frac{c_1^2}{2\langle c_1^2\rangle}\right\} \qquad \text{(GOE)}$$

Universal description of the interaction in a dot

$$\mathcal{H}_{int} = \frac{1}{2}\sum_{ss'}\sum_{ijkl} h_{ijkl}\, d_{is}^{+} d_{js'}^{+} d_{ks'} d_{ls}$$

$$h_{ijkl} = \int d\vec{r}\, d\vec{r}'\; \varphi_i^{*}(\vec{r})\varphi_j^{*}(\vec{r}')\, U(r-r')\, \varphi_k(\vec{r}')\, \varphi_l(\vec{r})$$

$\|\varphi\| = 1 \Rightarrow \quad h_{ijkl} \propto 1/L^{d}, \quad \dfrac{h_{ijkl}}{\delta E} \propto L^{0}$

$\langle \varphi_i \varphi_j \rangle \sim \delta_{ij}$ (RMT) $\Rightarrow \langle h_{ijkl} \rangle = A\delta_{il}\delta_{jk} + B\delta_{ik}\delta_{jl} + C\delta_{ij}\delta_{kl}$

$C = 0$ (GUE, or repulsive U → no superconductivity)

Invariants: $\hat{N} = \sum_{ns} d_{ns}^{+} d_{ns}$, $\hat{S} = \sum_{nss'} d_{ns}^{+} \dfrac{\sigma_{ss'}}{2} d_{ns'}$

$$\mathcal{H}_U = E_c (\hat{N} - N_0)^2 - E_s \hat{S}^2 , \qquad N_0 = \frac{1}{e} C_g V_g$$

valid for $|\varepsilon| \lesssim E_T$, but for evaluation of E_c, E_s states with $|\varepsilon_i - \varepsilon_j| \sim r_s E_F \gg E_T$ are important (RPA)

$$E_c \sim e^2/L$$

$$E_s = \int d\vec{r}\, d\vec{r}'\; U_{scr}(\vec{r}-\vec{r}') \langle \varphi_i(\vec{r})\varphi_i^{+}(\vec{r}') \rangle^2 \sim \delta E \cdot r_s \cdot \ln \frac{1}{r_s^2} \quad \text{(2DEG)}$$

$$\langle \varphi_i(\vec{r}_1)\varphi_j(\vec{r}_2) \rangle = \frac{\delta_{ij}}{L^2} F(|\vec{r}_1 - \vec{r}_2|); \quad F(|\vec{r}|) \sim \langle e^{i\vec{k}\vec{r}} \rangle_{FS}$$

$$\mathcal{H}_{dot} = \sum_{ns} \xi_n d^+_{ns} d_{ns} + E_c(\hat{N} - N_0)^2 - E_s \hat{S}^2 + \text{small } (\tfrac{1}{g}) \text{ corrections}$$

$\sim \delta E$ $\quad$ $\sim E_c$ $\quad$ $\sim r_s \delta E$ $\quad$ $\mathcal{H}^{1/g}$

Leading terms in $\mathcal{H}^{1/g}$ for 2D dot: $\dfrac{\delta E}{\sqrt{g}} \propto \dfrac{\delta E}{\sqrt[4]{N}}$

(Blanter, Mirlin, Muzykantskii 97)

$\dfrac{E_c}{E_T} \sim r_s$ in a ballistic ($\ell \sim L$) dot

Statistics of energy levels:

* electron addition spectrum
* excitations at fixed N

Zeeman effect in the distribution function

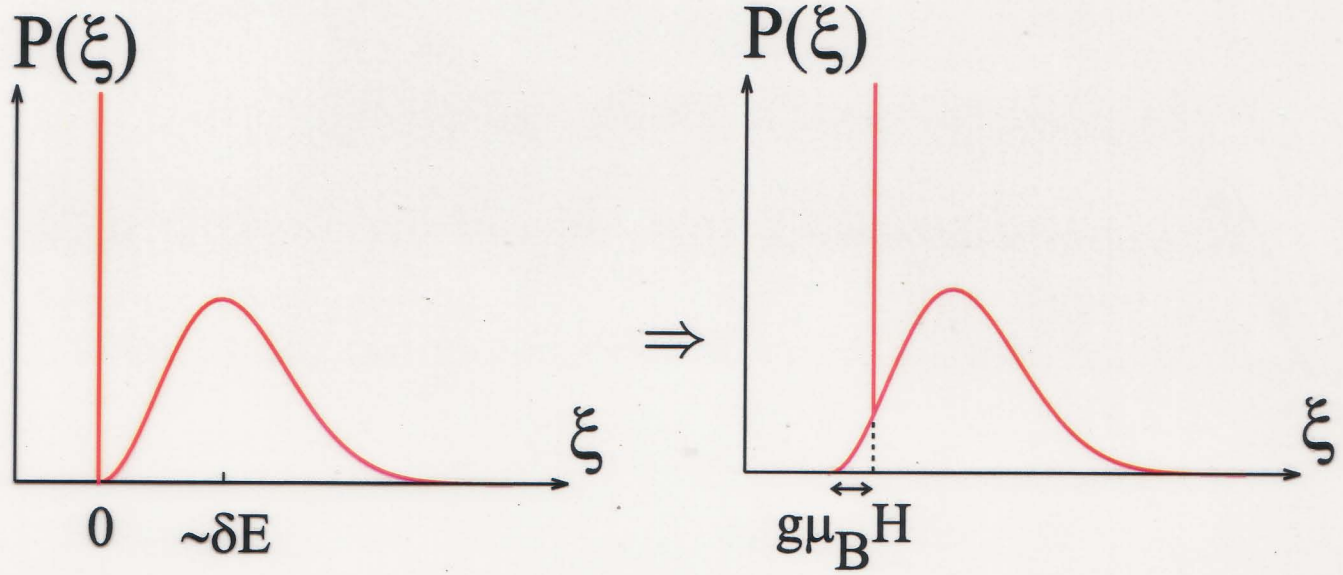

no spin-orbit interaction

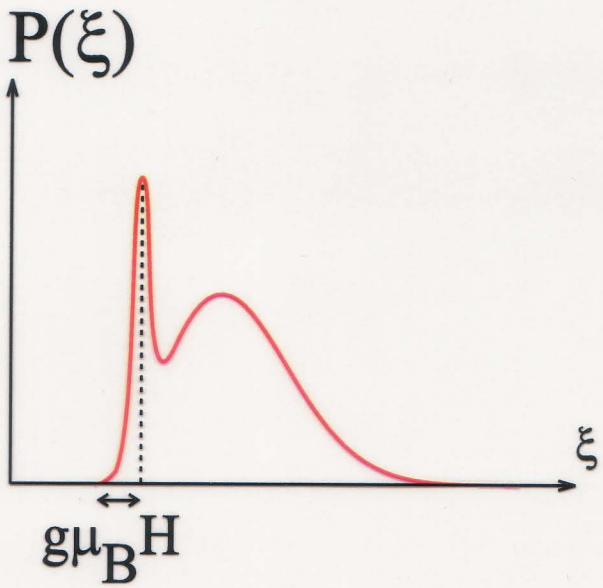

with the spin-orbit interaction

valid for relatively weak magnetic fields

(maxima of $P(\xi)$ do not overlap)

Effects of spin-orbit interactions on tunneling via discrete energy levels in metal nanoparticles

D. G. Salinas, S. Guéron, and D. C. Ralph
Laboratory of Atomic and Solid State Physics, Cornell University, Ithaca, New York 14853

C. T. Black
IBM Thomas J. Watson Research Center, Yorktown Heights, New York 10598

M. Tinkham
Department of Physics and Division of Applied Sciences, Harvard University, Cambridge, Massachusetts 02138

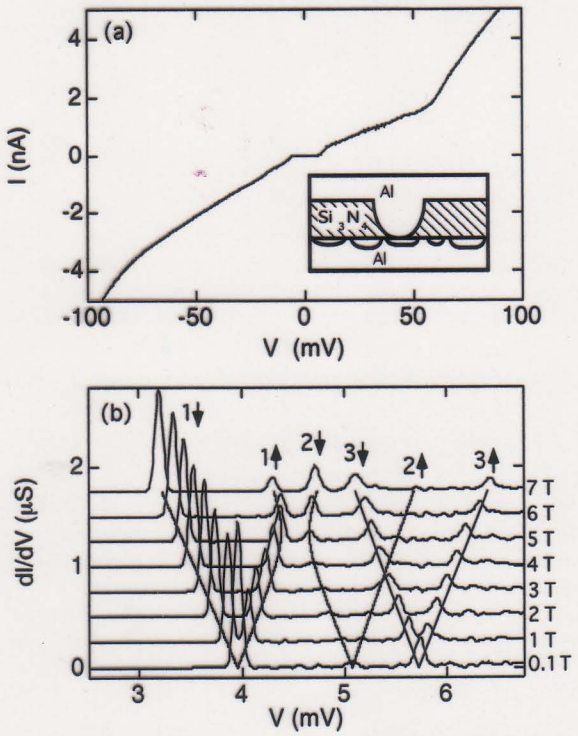

FIG. 1. (a) Large scale Coulomb-staircase curve for a tunneling device containing a nm-scale Al particle at $T = 50$ mK. Inset: Cross-sectional device schematic. (b) Tunneling spectrum of discrete state resonances in the same sample, for a range of applied magnetic fields, at $T = 50$ mK. The curves are offset in dI/dV for visibility. Orbital state #2 gives small but visible resonances at low B. Small changes in offset charge occurred between the 0.1 and 1 Tesla scans and between the 6 and 7 Tesla scans, shifting peak positions. The 0.1 and 7 Tesla scans have therefore been shifted along the voltage axis, to give the best fit to a linear dependence for peak 1 ↓. The lines tracing under peaks are guides to the eye.

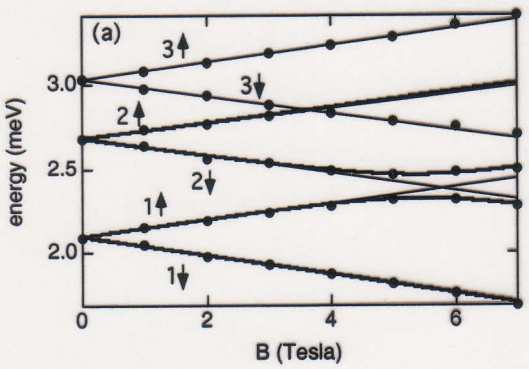

FIG. 2. (a) Energies of the discrete electronic states within the nanoparticle of Fig. 1, calculated by multiplying the voltage positions of the resonances by the capacitance ratio $eC_1/(C_1 + C_2) = e\ 0.53$. The thin lines are extensions of the low-field linear dependence of the energies on B. Heavy lines show the result of the spin-orbit interaction model, describing the avoided crossing between levels 1 ↑ and 2 ↓.

$g_{eff} = 1.84; 1.68; 1.76 < 2$

Only 4% of Au: $g_{eff} \approx 0.7$

Au particles: $g_{eff} \approx 0.3$

(Davidović + Tinkham, PRL199

- How the position of the Zeeman peak depends on the SO interaction?
  (modification of $\langle g \rangle$)
- How the width of the Zeeman peak depends on the SO interaction?
  (appearance of $\langle g^2 \rangle - \langle g \rangle^2 \neq 0$)

Splitting of the individual levels:

$\varepsilon_{i\sigma}(H) = \varepsilon_i \pm \frac{1}{2} g_i \mu_B H_z$

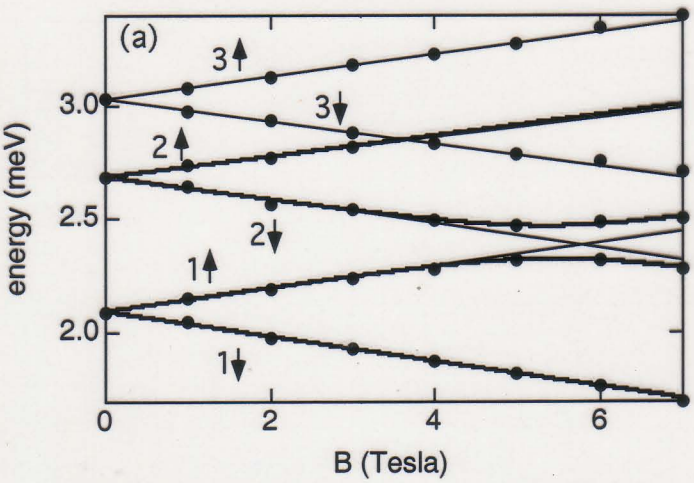

To characterize the strength of the SO interaction, we introduce (size-independent) SO relaxation rate

$$\frac{1}{\tau_{so}} = \frac{2\pi}{\hbar} \sum_{p,\beta} |\langle k, \alpha | \mathcal{H}_{so} | p, \beta \rangle|^2 \delta(\varepsilon_k - \varepsilon_p)$$

General property of SO interaction (T-invariance):

$$\langle k, \alpha | \mathcal{H}_{so} | k, \beta \rangle = 0$$

Perturbative correction to the $g = 2$ value:

$$\delta g_i \sim \frac{1}{\mu_B} \frac{\partial}{\partial H} \sum_j \frac{|\langle i, \alpha | \mathcal{H}_{so} | j, \beta \rangle|^2}{\varepsilon_i - \varepsilon_j - \mu_B H} \Bigg|_{H \to 0} \sim \frac{1}{\tau_{so} \delta E}$$

Rigorous calculation:

$$\langle g \rangle = 2 - \frac{\pi}{6} \frac{\hbar}{\tau_{so} \delta E} \ln \left(\frac{\tau_{so} \delta E}{\hbar} \right)$$

Weak or strong SO interaction:
Parameter $\lambda = \frac{\hbar}{\tau_{so} \delta E}$ small or large.

Meaning of λ:

τ_{so}: time between the spin flips;

$\hbar / \delta E$: travel time along the trajectory corresponding to a quantum level

λ is the typical number of spin flips for such a trajectory

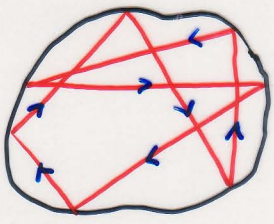

Strong SO interaction ($\lambda \gg 1$)

Magnetic moment of a state i:

$$\langle M \rangle_i = \mu_B \left(\langle l_z \rangle_i + 2 \langle s_z \rangle_i \right)$$

At $\lambda \neq 0$, the angular momentum $\langle l_z \rangle_i \neq 0$, even in the limit $H \Rightarrow 0$.

(Kravtsov, Zirnbauer, PRB 1992)

Level splitting at $H \neq 0$:
effect of perturbation $\mathcal{H}_1 = MH$

Two contributions to g

Estimate of the spin contribution to g:
Number of spin flips is large, $rms\ spin \sim \frac{1}{\sqrt{\lambda}}$

Spin splitting in the field: $\sim \mu_B \frac{1}{\sqrt{\lambda}} H$

$$g_{sp} \sim \sqrt{\tau_{so} \delta E / \hbar}$$

$$\delta E \sim 1/\nu L^d$$

g_{sp} scales with size L as $g_{sp} \propto \begin{cases} 1/L^{3/2}, & d = 3 \\ 1/L, & d = 2 \end{cases}$

Estimate of the orbital contribution to g:

At $\lambda \gtrsim 1$: $|\langle l_z \rangle_i| \sim \sqrt{\langle l_z^2 \rangle_i}\,|_{\lambda=0}$

$$\sqrt{\langle l_z^2 \rangle_i} \sim |(\vec{r}\times\vec{p})_z| \sim m\left|(\vec{r}\times\frac{d\vec{r}}{dt})_z\right| \sim \frac{\left|\oint \vec{r}\times d\vec{l}\right|}{\int_0^{\hbar/\delta E} dt} = m\mathcal{A}\delta E/\hbar$$

$\mathcal{A}$: directed area under the trajectory,

$$\mathcal{A} \sim L^2\sqrt{\frac{E_T}{\delta E}} \quad \left(\sim L^2\sqrt{\frac{Dt}{L^2}}\right)$$

sign is random.

$$\langle l_z \rangle_i = mL^2\sqrt{E_T \delta E} \sim \begin{cases} \sqrt{l/L}, & d=3 \\ \sqrt{k_F l}, & d=2 \end{cases}$$

Orbital contribution to g

$$g_{orb} \sim \begin{cases} \sqrt{l/L}, & d=3 \\ \sqrt{k_F l}, & d=2 \end{cases}$$

The spin and orbital contributions to g are independent. In the $d=3$ case:

$$\langle g^2 \rangle = \frac{6}{\pi\hbar}\tau_{so}\delta E + \alpha\frac{l}{L}$$

g-factor and $1/\tau_{so}$ from ESR

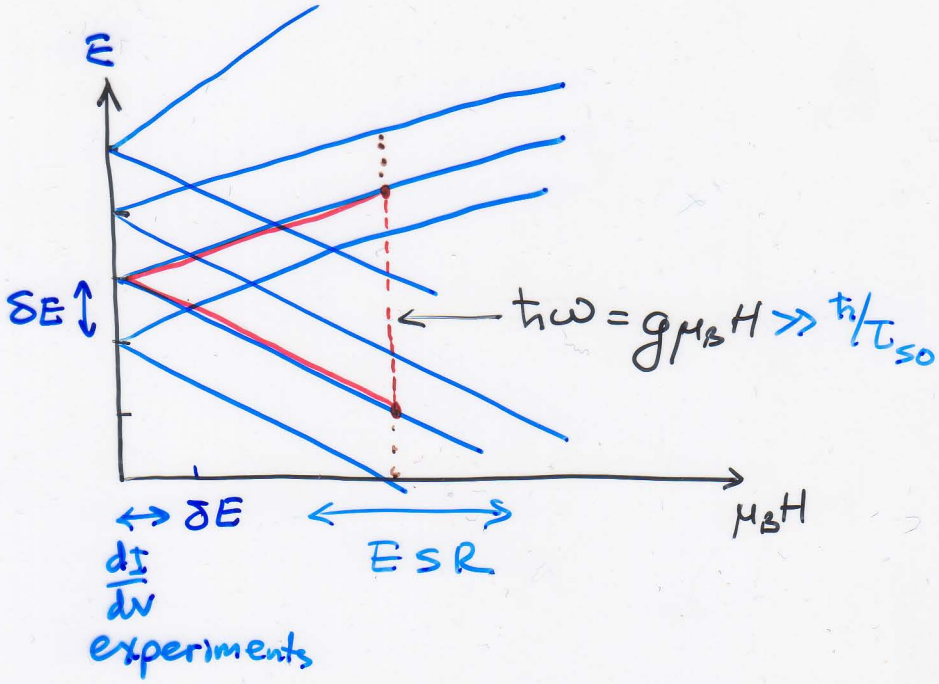

Coulomb blockade peak positions

I "~~Universal~~" model ($r_s \ll 1$):

$$\mathcal{H} = \mathcal{H}_{\rm free} + \mathcal{H}_{\rm int}, \qquad \mathcal{H}_{\rm int} = E_C(\hat{N} - \mathcal{N})^2;$$

$$\mathcal{H}_{\rm free} = \sum_{n,\sigma} \xi_n a^\dagger_{n\sigma} a_{n\sigma}.$$

Bimodal distribution: each orbital level ξ_n accomodates two electrons with *opposite* spins

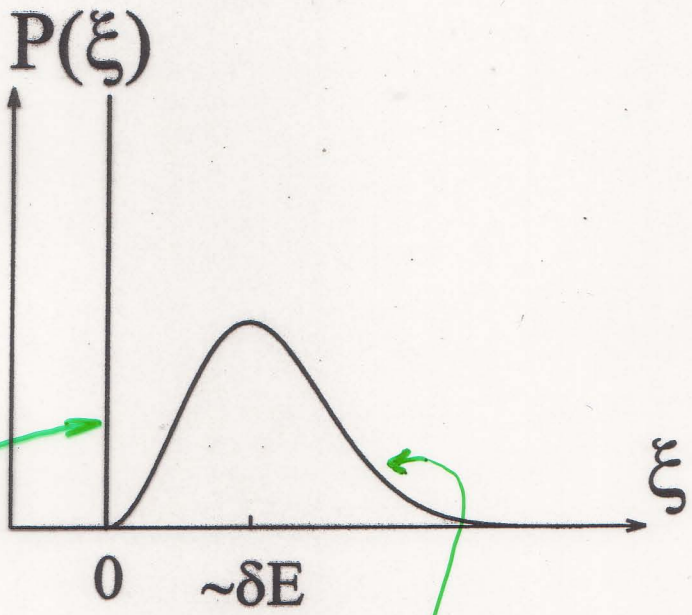

δ-peak: adding e to the same orbital level

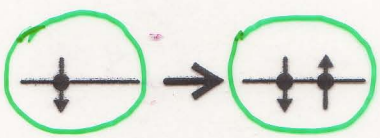

P_{WD}: Wigner-Dyson distribution for adding e to the next orbital level

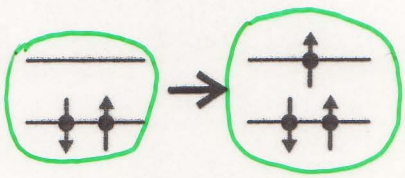

$$\mathcal{H}_{CI} = \sum_n \xi_n d^+_{n\sigma} d_{n\sigma} + E_c (\hat{N} - N)^2$$

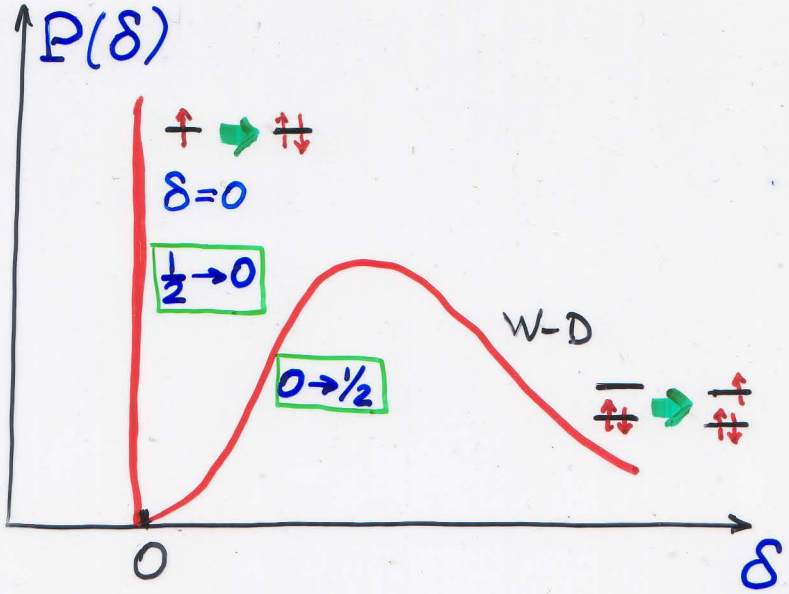

$$\mathcal{H}_{CIE} = \sum_n \xi_n d^+_{n\sigma} d_{n\sigma} + E_c (\hat{N} - N)^2 + E_s S^2$$

$E_s \sim \delta E \, r_s \ln \frac{1}{r_s}$

$E_s > 0$

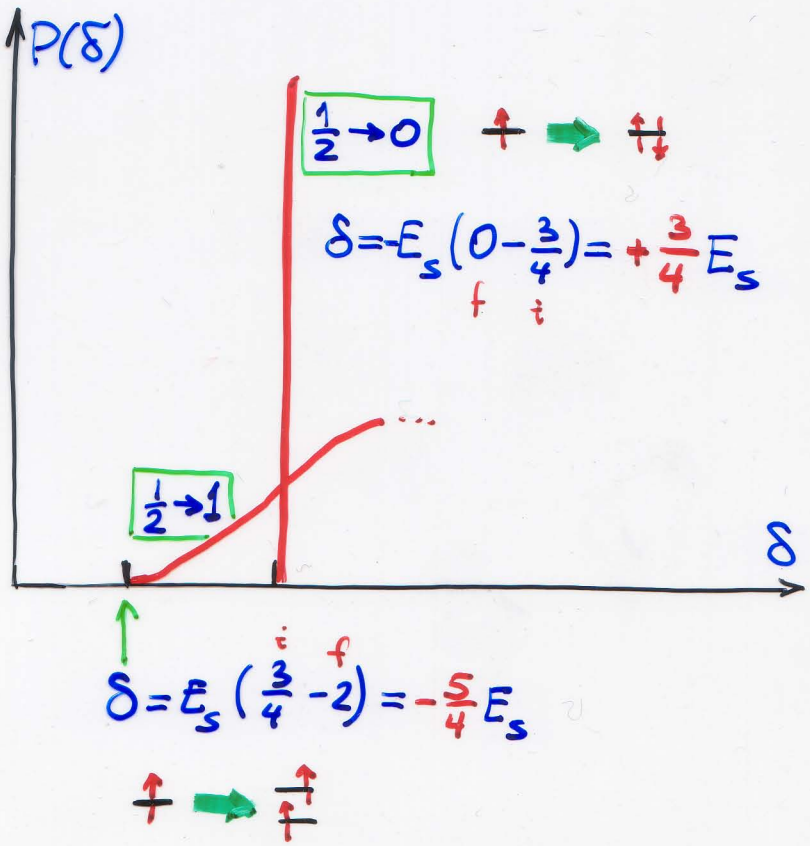

Signatures of spin pairing in a quantum dot in the Coulomb blockade regime

S. Lüscher[1], T. Heinzel[1], K. Ensslin[1], W. Wegscheider,[2,3] and M. Bichler[3]
[1] *Solid State Physics Laboratory, ETH Zürich, 8093 Zürich, Switzerland*
[2] *Institut für Angewandte und Experimentelle Physik, Universität Regensburg, 93040 Regensburg, Germany*
[3] *Walter Schottky Institut, TU München, 85748 Garching, Germany*
(February 15, 2000, cond-mat/0002226)

Coulomb blockade resonances are measured in a GaAs quantum dot in which both shape deformations and interactions are small. The parametric evolution of the Coulomb blockade peaks shows a pronounced pair correlation in both position and amplitude, which is interpreted as spin pairing. As a consequence, the nearest-neighbor distribution of peak spacings can be well approximated by a smeared bimodal Wigner surmise, provided that interactions which go beyond the constant interaction model are taken into account .

PACS numbers: 73.20.My, 73.23.Hk, 05.45.+b

$$P(s) = \frac{1}{2}\left[\delta(s) + P^{\beta}(s)\right] \qquad (1)$$

$P^{\beta}(s)$ is the Wigner surmise for the corresponding Gaussian ensemble, i.e. $\beta = 1$ for systems with time inversion symmetry (Gaussian orthogonal ensemble - GOE), and $\beta = 2$ when time inversion symmetry is broken (Gaussian unitary ensemble - GUE). The peak spacing s is measured in units of the average spin-degenerate energy level spacing.

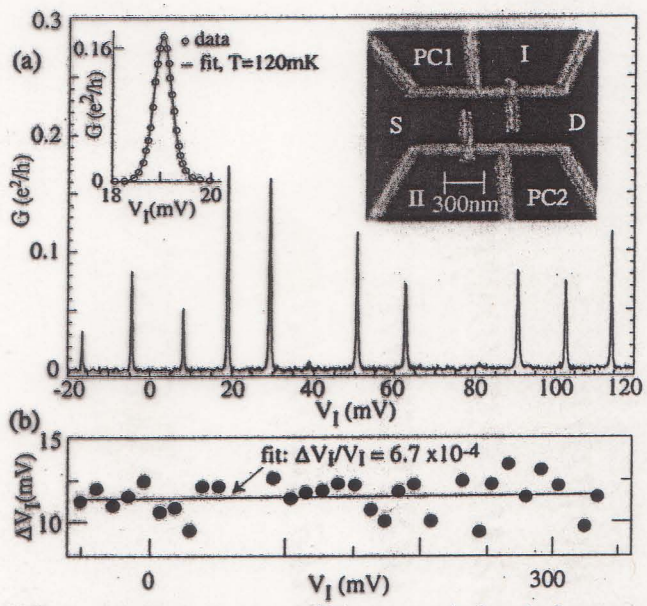

FIG. 1. (a) Right inset: AFM picture (taken before evaporation of the top gate) of the oxide lines (bright) that define the dot, coupled to source (S) and drain (D) via tunnel barriers, which can be adjusted with the planar gates PC1 and PC2. Gates I and II are used to tune the dot. Main figure: Conductance G as a function of V_I, showing Coulomb blockade resonances. Left inset: fit (line) to one measured CB peak (open circles), see text. (b) Linear fit (line) of the peak spacing ΔV_I as a function of V_I (dots). The average peak spacing is almost constant, indicating small shape deformations.

$$P^{\beta}_{int}(\overline{\xi^*}, \sigma_{\xi^*}) = \frac{1}{\sqrt{2\pi}\sigma_{\xi^*}}\left\{exp\left[-\frac{(s-\overline{\xi^*})^2}{2\sigma^2_{\xi^*}}\right] + exp\left[-\frac{s^2}{2\sigma^2_{\xi^*}}\right] \times P^{\beta}(s+\xi^*)\right\} \qquad (2)$$

Here, the "×" denotes the convolution.

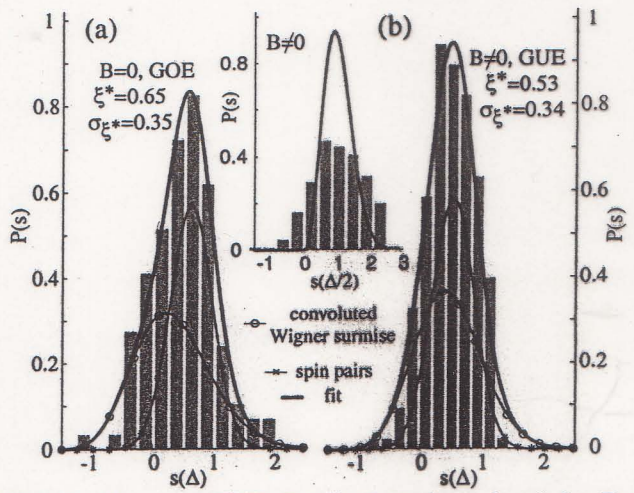

FIG. 2. Measured NNS distributions (gray bars) for B=0 (a) and B ≠ 0 (b). The bold solid curves are the fits to $P^{\beta}_{int}(\overline{\xi^*}, \sigma_{\xi^*})$, with the fit results as indicated in the figure (see text). Also drawn are the two components of P^{β}_{int}, i.e. the Gaussian distribution of separations between spin pairs, and its convolution with the corresponding Wigner surmises. The inset compares the GUE data to $P^2(s)$ (eq. 1), using the spin-resolved level spacing $\Delta/2$ as the average peak separation.

[1] For a review, see L.P. Kouwenhoven, C.M. Marcus, P.L. McEuen, S. Tarucha, R.M. Westervelt, and N.S.

Resonant tunneling through a single level

$$G = \frac{2e^2}{2\pi\hbar} \int d\varepsilon \left(-\frac{\partial f_F}{\partial \varepsilon}\right) \frac{4\Gamma_l \Gamma_r}{(\Gamma_l+\Gamma_r)^2 + (\varepsilon-\varepsilon_0)^2}$$

Fluctuations of conductance through a quantum dot

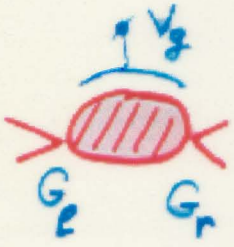

$$G_l, G_r \ll \frac{e^2}{h}$$

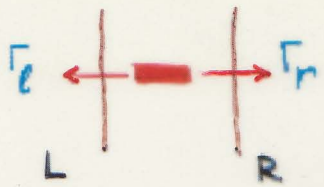

Low temperatures ($T \lesssim \delta E$) ⇒ narrow peaks in the conductance,

$$G_{max} = \frac{e^2}{4h} \frac{\Gamma_l \Gamma_r}{(\Gamma_l + \Gamma_r) T} \equiv \frac{e^2}{4hT} \cdot \Gamma$$

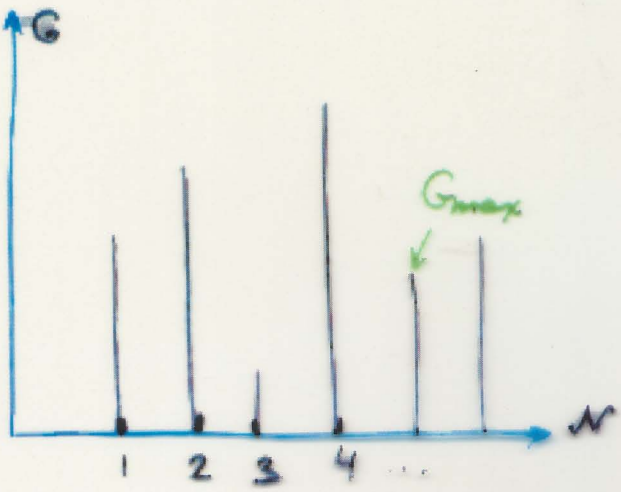

$$\langle \Gamma_i \rangle = \frac{\hbar}{e^2} G_i \cdot 2\delta E \qquad i = l, r$$

but: $\Gamma_i \propto |\psi_n(R_i)|^2$,

and fluctuates (Porter-Thomas, 1956)

$$P(\Gamma) = \int d\Gamma_l \, d\Gamma_r \; P_{PT}(\Gamma_l) \, P_{PT}(\Gamma_r) \, \delta\left(\frac{\Gamma_l \Gamma_r}{\Gamma_l + \Gamma_r} - \Gamma\right)$$

Non-Gaussian Distribution of Coulomb Blockade Peak Heights in Quantum Dots

A. M. Chang,[1] H. U. Baranger,[1] L. N. Pfeiffer,[1] K. W. West,[1] and T. Y. Chang[2]
[1]*AT&T Bell Laboratories, 600 Mountain Avenue, Murray Hill, New Jersey 07974-0636*
[2]*AT&T Bell Laboratories, Crawfords Corner Road, Holmdel, New Jersey 07733*
(Received 26 July 1995)

We have observed a strongly non-Gaussian distribution of Coulomb blockade conductance peak heights for tunneling through quantum dots. At zero magnetic field, a low-conductance spike dominates the distribution; the distribution at nonzero field is distinctly different and still non-Gaussian. The observed distributions are consistent with theoretical predictions based on single-level tunneling and the concept of "quantum chaos" in a closed system weakly coupled to leads.

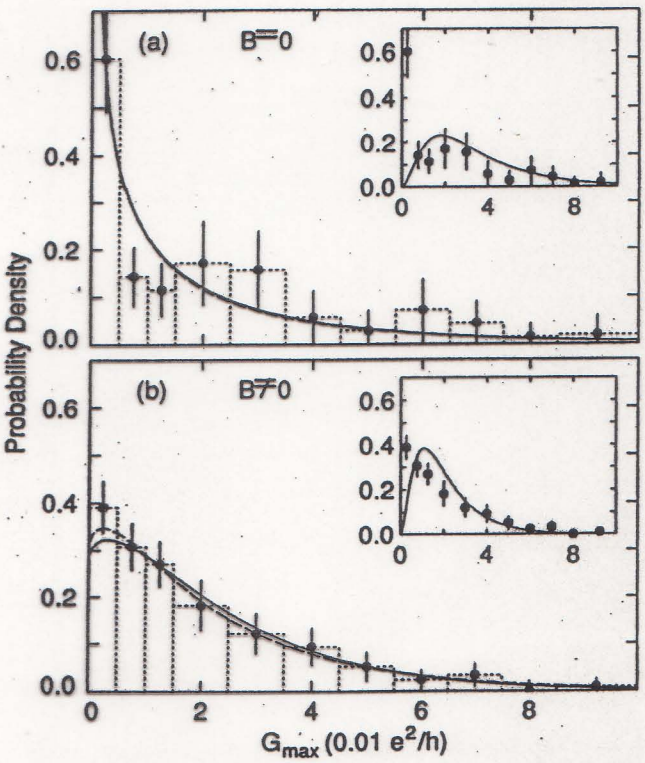

G. 4. Histograms of conductance peak heights for (a) $B =$ and (b) $B \neq 0$. Data are scaled to unit area; there are ! peaks for $B = 0$ and 216 peaks for $B \neq 0$; the statistical ror bars are generated by bootstrap resampling. Note the n-Gaussian shape of both distributions and the strong spike ar zero in the $B = 0$ distribution. Fits to the data using both e fixed pincher theory (solid) and the theory averaged over ncher variation (dashed) are excellent. The insets show fits $\chi^2_6(\alpha)$—a more Gaussian distribution—averaged over the ncher variation; the fit is extremely poor.

$$G_{max} = \frac{e^2}{h}\frac{\pi\bar{\Gamma}}{2kT}\alpha$$

$$P(\alpha) = \sqrt{\frac{2}{\pi\alpha}}\, e^{-2\alpha} \qquad \text{GOE } (B=0)$$

$$P(\alpha) = 4\alpha[K_0(2\alpha) + K_1(2\alpha)]e^{-2\alpha} \qquad \text{GUE } (B>B_c)$$

(Jalabert, Stone, Alhassid, 1992)

Multichannel case:
Mucciolo, Prigodin, Altshuler, 1995

Crossover GOE → GUE:
Falko, Efetov, 1996

Experiment

Statistics and Parametric Correlations of Coulomb Blockade Peak Fluctuations in Quantum Dots

J. A. Folk, S. R. Patel, S. F. Godijn, A. G. Huibers, S. M. Cronenwett, and C. M. Marcus
Department of Physics, Stanford University, Stanford, California 94305-4060

K. Campman and A. C. Gossard
Materials Department, University of California at Santa Barbara, Santa Barbara, California 93106
(Received 18 September 1995)

We report measurements of mesoscopic fluctuations of Coulomb blockade peaks in a shape-deformable GaAs quantum dot. Distributions of peak heights agree with predicted universal functions for both zero and nonzero magnetic fields. Parametric fluctuations of peak height and position, measured using a two-dimensional sweep over gate voltage and magnetic field, yield autocorrelations of height fluctuations consistent with a predicted Lorentzian-squared form for the unitary ensemble. We discuss the dependence of the correlation field on temperature and coupling to the leads as the dot is opened.

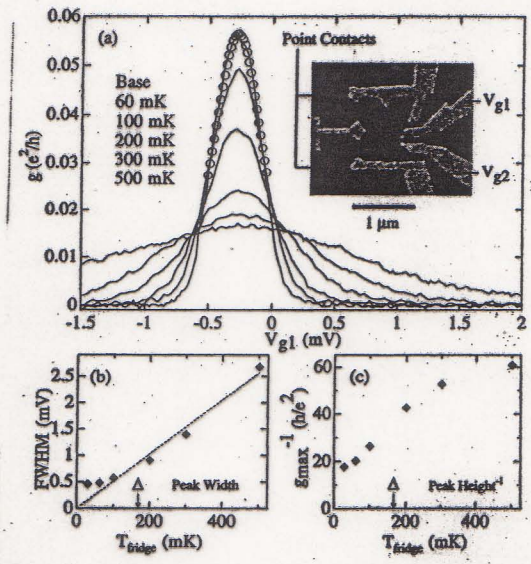

FIG. 1. (a) Temperature dependence of Coulomb peak line shape for the larger dot ($\Delta = 15\ \mu$eV). Circles show fit of base temperature peak by $g/g_{max} = \cosh^{-2}(\eta eV_g/2kT)$. Inset: Micrograph of the larger dot. V_{g1} and V_{g2} are shape distorting gates. (b) Peak width measured as FWHM of the fit to $\cosh^{-2}$. Linear behavior at high temperatures gives voltage-to-energy scale $\eta = 0.12$. (c) Inverse peak height decreases with temperature for $kT < \Delta$. From saturations at low T in (b) and (c) we estimate the electron temperature in the dot to be 70 ± 20 mK.

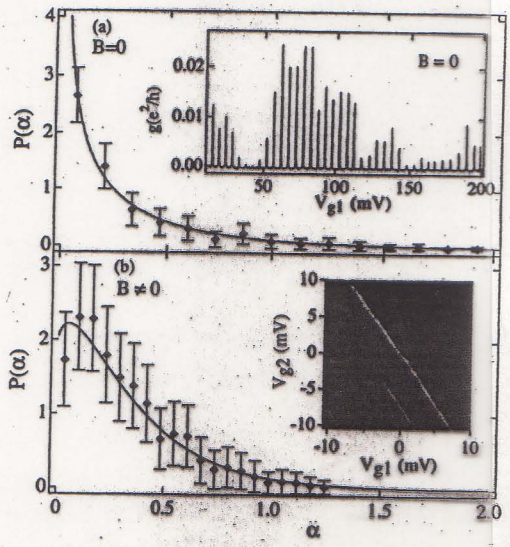

FIG. 2. Distribution of Coulomb peak conductances, scale to dimensionless conductances α [Eq. (2)] for (a) the orthogonal ($B = 0$) ensemble and (b) the unitary ensemble ($B \neq 0$). Insets: (a) Example of a set of peaks from which the distribution was obtained. (b) Grayscale plot of small region of gate-gate sweep used to derive these distributions, showing Coulomb "ridges" along lines of constant area (lighter = higher conductance). Error bars assume ~90 statistically independent samples (see text).

$P(\alpha) = \sqrt{\frac{2}{\pi\alpha}}\, e^{-2\alpha}$ GOE (B=0)

(Jalabert, Stone, Alhassid, 1992)

$\Phi_c^{exp} > \Phi_0/\sqrt{E_t/\delta E}$

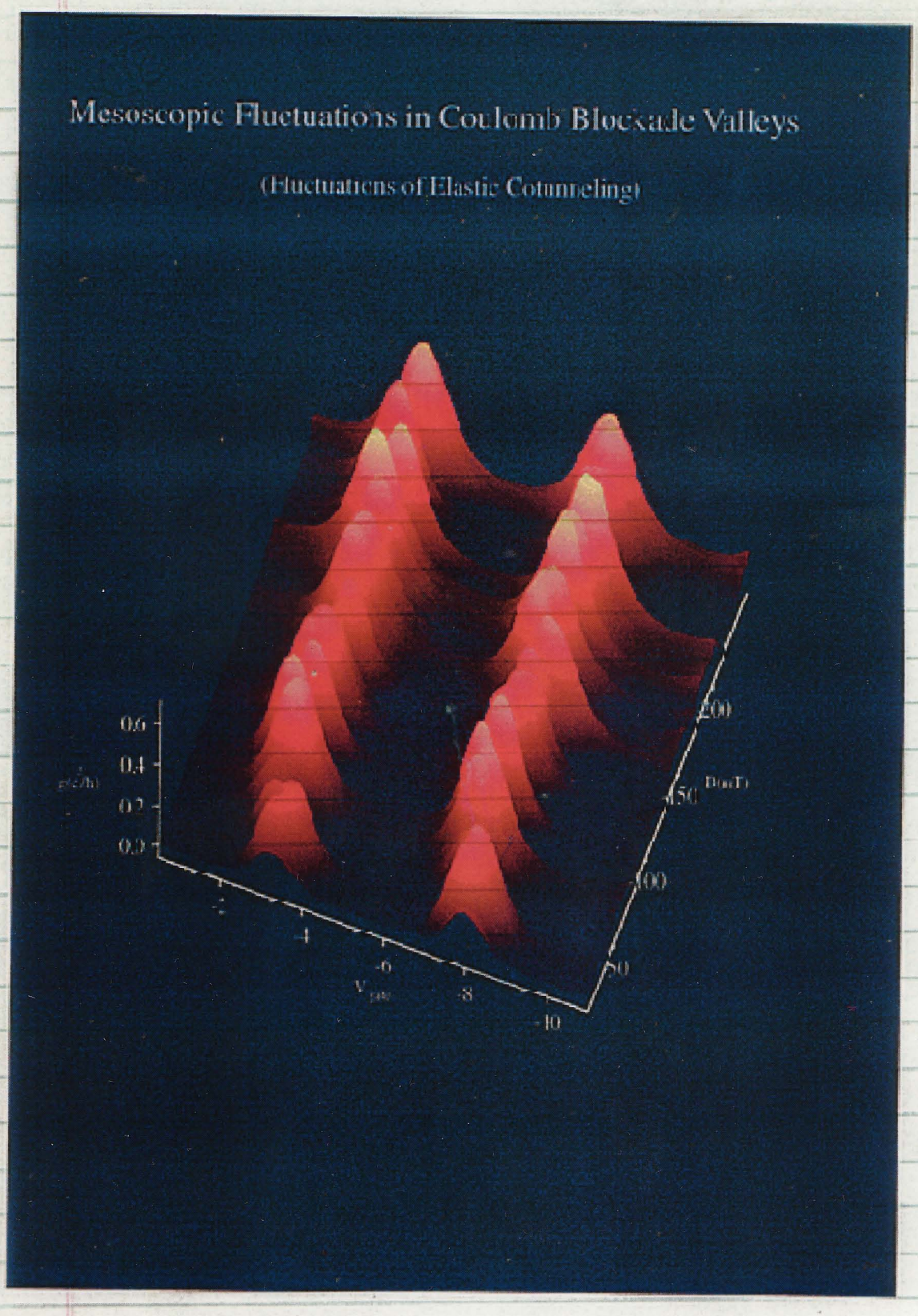
Mesoscopic Fluctuations in Coulomb Blockade Valleys
(Fluctuations of Elastic Cotunneling)
0.6
0.4
0.2
0.0
-4
-6
-8
-10
200
150
100
50

Higher-order tunneling processes (co-tunneling)

* Inelastic co-tunneling (Averin, Odintsov 88)

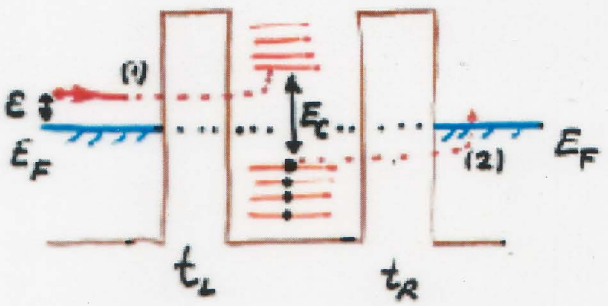

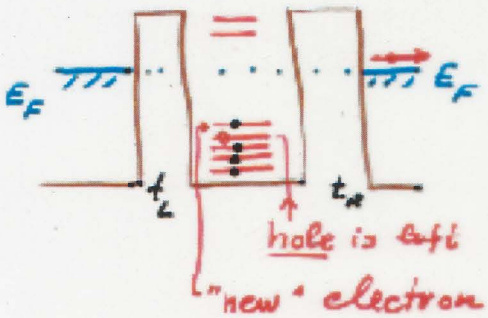

$$\delta E \ll \varepsilon \ll E_c$$

$$A_{in} \propto \frac{t_L t_R}{E_c} \Rightarrow$$

e-h phase space $\propto T^2$ $\Rightarrow$

$$G_{in} \propto |A_{in}|^2 T^2 \sim \frac{G_L G_R}{e^2/h}\left(\frac{T}{E_c}\right)^2$$

$$G_{in} \gg G_{act.} \iff T \lesssim \frac{E_c}{\ln\left(\frac{e^2/h}{G_L+G_R}\right)}$$

* Elastic co-tunneling (Averin, Nazarov 91; Aleiner, L.G. 96)

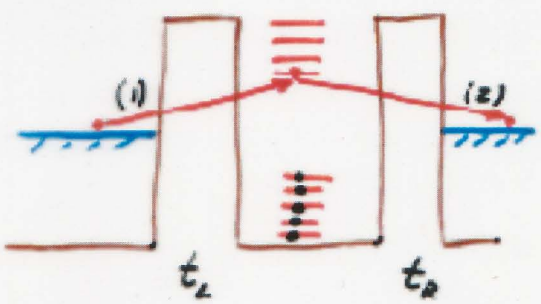

$$\langle G_{el} \rangle \sim \frac{G_L G_R}{e^2/h} \cdot \frac{\delta E}{E_c}$$

$$G_{el} \gtrsim G_{in} \iff T \lesssim \sqrt{E_c \delta E}$$

Elastic co-tunneling: contributions of many levels to the tunneling amplitude

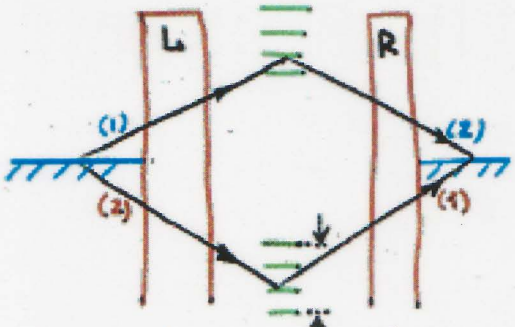

# of participating levels: $N \sim E_c/\delta E$

$$A = \sum_{i=1}^{N} A_i$$

$$A_i \propto \frac{\psi_i(r_L)\,\psi_i^*(r_R)}{E_c + |\xi_i|}$$

Random $\psi_i \Rightarrow$ random A_i

$$\langle |A_i|^2 \rangle \sim \frac{\Gamma_{i\to L}\cdot\Gamma_{i\to R}}{E_c^2} \sim \left[\frac{h}{e^2}\right]^2 G_L G_R \left(\frac{\delta E}{E_c}\right)^2$$

$$|A|^2 = \underbrace{\sum_{i=1}^{N} |A_i|^2}_{N \text{ terms}} + \underbrace{\sum_{i\neq j}^{N} A_i A_j^*}_{N^2-N \text{ terms}}$$

$$\langle |A|^2 \rangle = N \cdot \langle |A_i|^2 \rangle \qquad \text{var}\,|A|^2 \sim \sqrt{N^2-N}\,\langle |A_i|^2 \rangle$$

$$N \gg 1 \Rightarrow \quad \langle |A|^2 \rangle \sim \text{var}\,|A|^2$$

$$\langle G_{el} \rangle \simeq \sqrt{\langle (\delta G_{el})^2 \rangle} \sim \left(\frac{h}{2e}\right)^2 G_L G_R \frac{\delta E}{E_c}$$

Averin, Nazarov 1990 — Aleiner, L.G. 1996

Energy deficit E_c → many discrete levels participate in co-tunneling,

$N_{st} \sim E_c/\delta E$

Large magnetic flux is needed to change G_{el}

Variable gate voltage:

Energy deficit $E_c|N-N^*| \Rightarrow$ # of participating states: $N_{st} \sim \frac{E_c}{\delta E}|N-N^*|$

Smaller flux is needed to change conductance

$$\langle \delta G(B_1)\, \delta G(B_2)\rangle = \langle G_{el}\rangle^2 F\left(\frac{|B_1-B_2|}{B_c}\right)$$

$$B_c \sim \frac{\Phi_0}{S}\sqrt{\frac{E_c}{E_T}|N-N^*|}$$ - correlation field

$E_T = \hbar D/S$ - Thouless energy

B_c depends on gate voltage:

min G ⟷ max B_c

Rigorous theory: Aleiner, L.G. PRL (96)

(15)

OSCILLATION OF B_c – OUT OF PHASE WITH $\langle G \rangle$

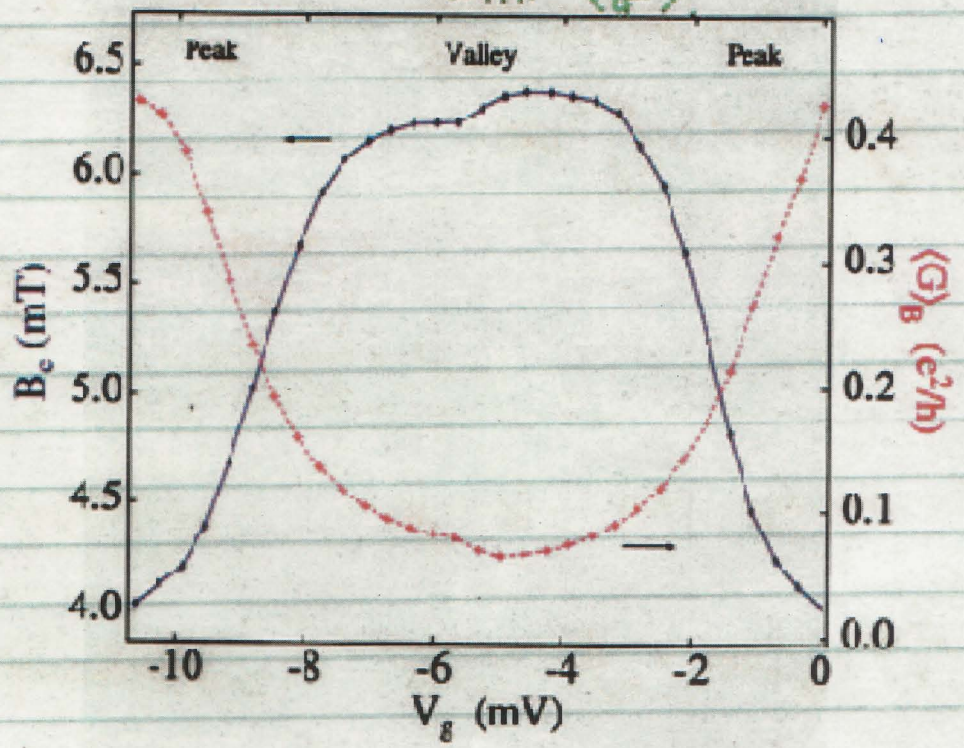

$B_c = k \frac{\phi_0}{A} \sqrt{\frac{E_L}{E_T}}$

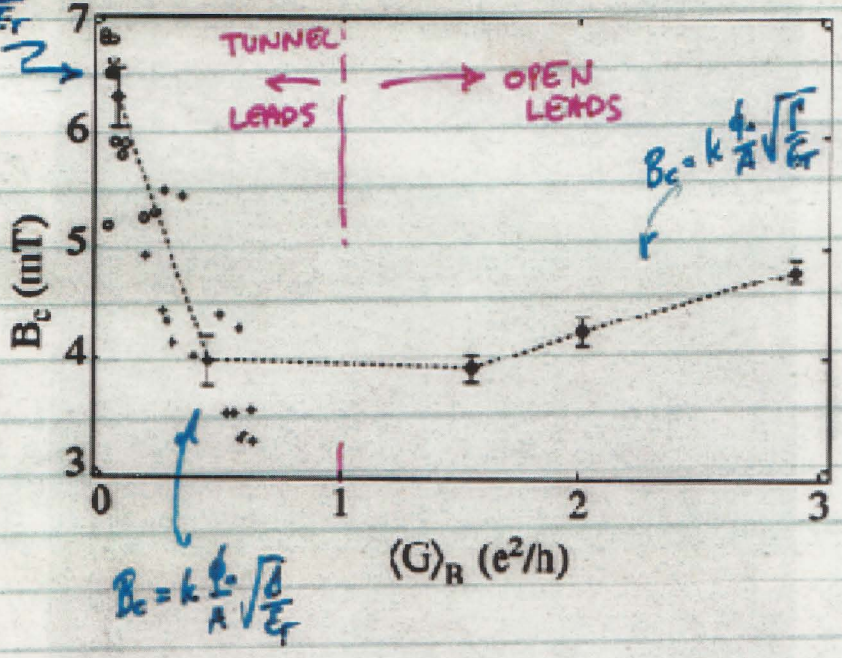

S. Cronenwett et. al., PRL 97

Conductance through a blockaded dot

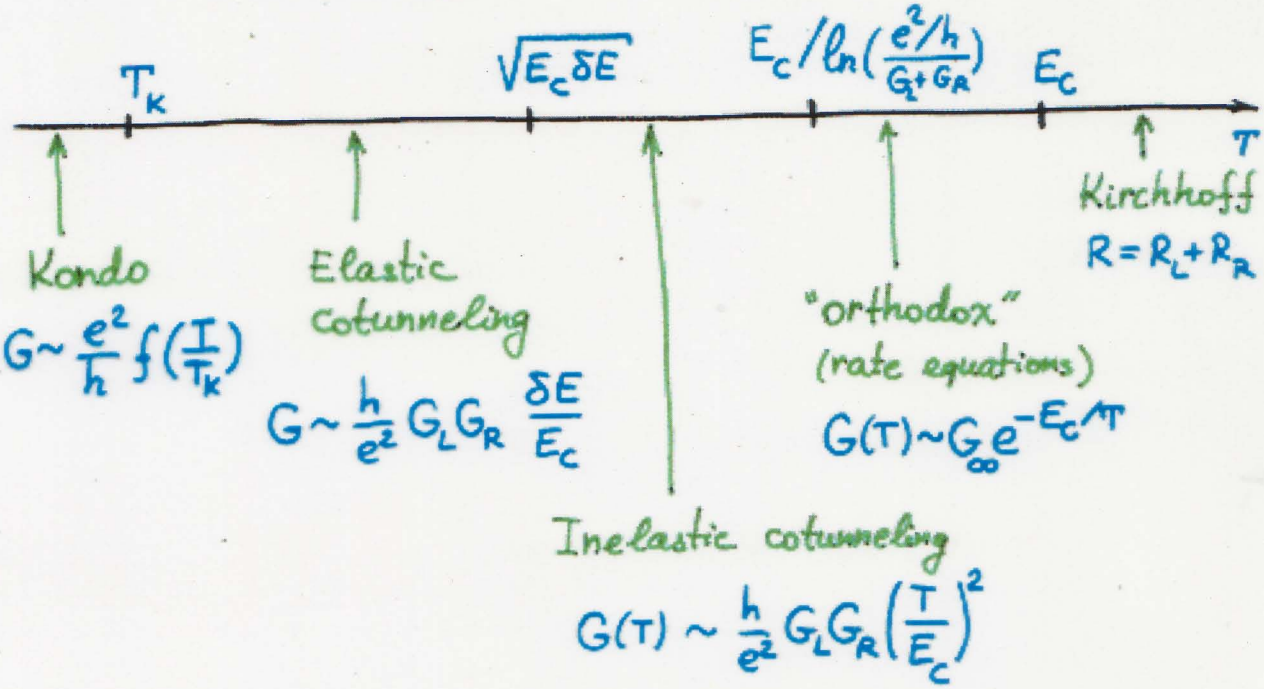

$$\frac{\delta E}{E_C} \ll 1 ; \quad G_L, G_R \ll \frac{e^2}{h} ; \quad T_K \propto \exp\left\{-\frac{E_C}{\delta E} \cdot \frac{e^2/h}{G_L+G_R}\right\}$$

$G \sim \frac{e^2}{h}$ fluctuates $G \sim \frac{e^2}{h}\frac{\Gamma}{T}$

$G_L = G_R \equiv 2G_\infty \ll \frac{e^2}{h}$

$G_L, G_R \sim \frac{\langle\Gamma\rangle}{\langle\delta E\rangle} \cdot \frac{e^2}{h}$

$\Gamma \ll \delta E \ll E_c$

Kondo effect in the CI model.

Recall the elastic co-tunneling:

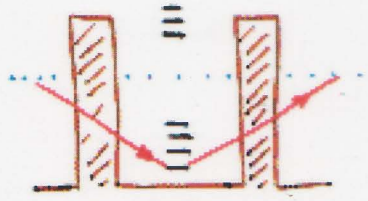

Involves $\sim \frac{E_c}{\delta E}$ virtual levels

Dot with odd electron number:

the top-most singly-occupied level is special

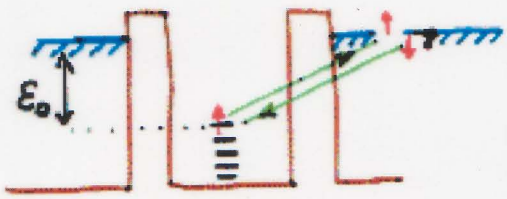

Can exchange spin with the itinerant electrons of the leads

Similar to the Anderson model of magnetic impurity:

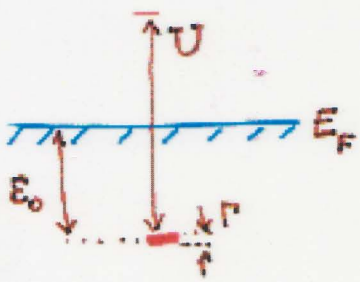

$$\mathcal{H}_A = \sum_{k\sigma} \xi_k c^+_{k\sigma} c_{k\sigma} + \sum_\sigma \varepsilon_0 d^+_\sigma d_\sigma + U n_\uparrow n_\downarrow + \sum_{k\sigma} t_k (c^+_{k\sigma} d_\sigma + d^+_\sigma c_{k\sigma})$$

Kondo Conductance

(Odd N, small r_s)

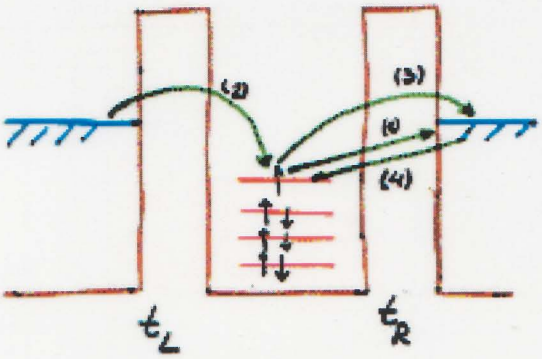

Starts with the 4-th order in $t_{L,R}$

(Amplitude $\propto \Gamma^2$)

But: singular: $\propto \ln \frac{E_c}{T}$

$$\mathcal{H} = \sum_{k\sigma} \varepsilon_{k\sigma} \left(c^+_{kL\sigma} c_{kL\sigma} + c^+_{kR\sigma} c_{kR\sigma} \right) + \sum_\sigma \varepsilon_0 d^+_{o\sigma} d_{o\sigma} + U n_\uparrow n_\downarrow$$

$$+ \sum_{k\sigma} \left\{ \left(t_L c^+_{kL\sigma} + t_R c^+_{kR\sigma} \right) d_{o\sigma} + d^+_{o\sigma} \left(t^*_L c_{kL\sigma} + t^*_R c_{kR\sigma} \right) \right.$$

$$\varepsilon_0 \simeq E_c \cdot (N - N') \; ; \quad U \sim E_c \; ; \quad \Gamma_{L,R} = \pi \nu_{L,R} \cdot |t_{L,R}|^2$$

Mapping on the Anderson impurity model:

$$\left\{ \begin{matrix} \alpha_{k\sigma} \\ \beta_{k\sigma} \end{matrix} \right\} = u c_{kL\sigma} \pm v c_{kR\sigma} \; ; \qquad \left\{ \begin{matrix} u \\ v \end{matrix} \right\} = \frac{1}{\sqrt{|t_L|^2 + |t_R|^2}} \left\{ \begin{matrix} t_L \\ t_R \end{matrix} \right\}$$

Band $\alpha_{k\sigma}$: like in the "usual" Anderson imp. model

L.G., Raikh 1988

Band $\beta_{k\sigma}$: free electrons

Summary

Large dots ($N \sim 10^2$) ~~N:~~ Gates estimates

1. Energy scales: $E_F \gg E_c \sim E_T \gg \delta E$
2. Energy levels: charging + exchange + RMT
3. Wave functions: RMT
4. Blockaded conductance ($\Gamma \ll \delta E$): peaks - single-level properties
   valleys - $E_c/\delta E$ states

Smaller dots ($N \sim 10$)

Spin (and level) degeneracies $\Rightarrow$ Kondo effect(s)
(Aug. 16-17)

Very small dots ($N \sim 1$)

Dynamics & relaxation of a single spin

Other subjects:

* superconducting grains, magnetic grains
* crossover to an open dot ($\Gamma \to \delta E$) and its conductance
* electron relaxation in a dot (EM fluctuations, phonons, nuclear spins...)